

US-98-07

October,1998

hep-th/9810256

Weyl Anomaly in Higher Dimensions and Feynman Rules in Coordinate Space

Shoichi ICHINOSE ¹ and Noriaki IKEDA^{† 2}

Physics Department, Brookhaven National Laboratory,
Upton, NY 11973, USA

and

[†]Research Institute for Mathematical Sciences
Kyoto University, Kyoto 606-01, Japan

Abstract

An algorithm to obtain the Weyl anomaly in higher dimensions is presented. It is based on the heat-kernel method. Feynman rules, such as the vertex rule and the propagator rule, are given in (regularized) coordinate space. Graphical calculation is introduced. The 6 dimensional scalar-gravity theory is taken as an example, and its explicit result is obtained.

PACS NO: 02.70.-c, 04.60.-m, 11.15.Bt, 11.25.Db, 11.30.-j

Keywords: Weyl anomaly, Higher dimensional field theories, Heat kernel, Feynman

¹ On leave of absence from Department of Physics, University of Shizuoka, Yada 52-1, Shizuoka 422, Japan (Address after Nov.6, 1998).

E-mail address: ichinose@u-shizuoka-ken.ac.jp

² E-mail address: nori@kurims.kyoto-u.ac.jp

1 Introduction

The anomaly phenomenon is, as well as the renormalization, one of important aspects of the quantum field theories. It is a local quantum effect originating from regularization of the continuous space-time. We may say it is the problem of how to define the space-time as the continuum. Generally the symmetry, imposed at the classical level, does not hold at the quantum level due to the anomaly. As for the chiral anomaly, which is the anomaly concerned with the γ_5 -symmetry(chiral symmetry), the general form is well-established in arbitrary even dimensions [1]. It is fixed, except for an overall coefficient, by its cohomology structure and is given in a beautiful form in terms of the differential form: $\text{tr}(R \wedge R \wedge \dots \wedge R)$, $\text{tr}(F \wedge F \wedge \dots \wedge F)$. The topological nature due to the γ_5 -projection is the origin of its simplicity. On the other hand, as for the Weyl anomaly, the general form in higher dimensions is not so simple. This is the anomaly concerned with local scale transformations. Cohomology analysis restricts the Weyl anomaly to some extent, but there generally remains numerous candidate terms in higher dimensions[2]. The undetermined coefficients of those terms must be fixed in some way. The situation originates from the "rich" structure of the functional space on which the scale transformation acts. In the development of the string theory or M-theory, it becomes more and more necessary to investigate the Weyl anomaly in higher dimensional field theories[3]. At this circumstance we present a new formalism for it.

The Weyl anomaly itself is not harmful to the construction of physical theories because we know the realistic theories have some dimensional parameters, such as the mass or the cosmological constant, and they break the Weyl symmetry. However when we try to understand the origin of those massive parameters, the Weyl anomaly is so important because it triggers the symmetry breaking of the conformal invariant vacuum. In this sense the Weyl anomaly can be regarded as a "softer" anomaly than the chiral one. The latter threatens the consistency of the theory whereas the former does not. The nonrenormalization theorem is valid for the latter, whereas generally not for the former.

In supersymmetric theories, however, it is also known that both anomalies make a super multiplet together with the super current[4]. Under the supersymmetric treatment both anomalies are intimately related. In this connection there has been a lot of work. Because our interest here is to establish a general algorithm to treat the Weyl anomaly of the higher dimensional theories, we do not consider supersymmetry here. We suppose, using the present result, we can investigate how the Weyl anomaly is constrained by the supersymmetry.

We analyze the Weyl anomaly in the heat-kernel regularization. The content is essentially the same as, or overlaps with, topics with other names such as the effective action analysis, the background field method, the Schwinger-De Witt technique, Seeley series, etc. They all treat some background functional which represents (1-loop) quantum effects. It has a long history

since Schwinger[5], DeWitt[6] and Seeley[7]. Especially the first author, in 1951, treated quantum matter theories in external gauge fields keeping the gauge invariance of the effective action. He introduced an additional "coordinate" into the ordinary space(-time) coordinates, called "proper time" or "temperature" in a natural way. It was exploited by Alvarez-Gaumé and Witten [1] in the modern problem of the chiral anomaly of the gravitational theories. Later it was generalized to the Weyl anomaly by a SUNY group [8, 9].

The effective action has been analyzed in various ways. Its divergent part was systematically and algorithmically analyzed by t'Hooft[12] in 1973 and with Veltman[13] in 1974 using dimensional regularization. As will be shown later, the Weyl anomaly is obtained from the "heat-kernel", which is the 1-loop effective action with the proper time as the ultraviolet regularization. The evaluation of the heat-kernel has been well-developed by many people [7, 14, 15, 16, 17, 10, 11, 18]. Each of them has their own characteristic formalisms. Generally they start with expressing a differential operator by some general background quantities. Most of them put emphasis on the covariance in the formulae in the intermediate stages. As originally done by t'Hooft[12], the "intermediate covariance" is powerful as far as the lower-order calculations, such as the heat-kernel on 2 and 4 dimensions, are concerned. However, at higher-order (this means higher dimensions too), it hinders one from performing explicit calculations because many more "intermediate invariants" appear than those appearing in the final explicit answer. The important thing is not the formulae at intermediate stages, but the final explicit result. Aiming at the treatment of the Weyl anomaly in higher dimensions, we present a new algorithm which is based on a simple weak-field expansion. Of course, we assume the invariance of the general coordinate and gauge symmetries at the final result, because it is guaranteed by the background (effective action) formalism [6, 12, 19].

The following are new points of the present approach:

1. We take a formalism in the regularized coordinate space, that is the space with the ordinary space(-time) coordinates and the proper time[20]. The Feynman rules in the coordinate space are given for the anomaly (effective action) calculation[21]. The ultraviolet regularization is done with the Schwinger's parameter (proper time). The regularization lets us properly evaluate both chiral and Weyl anomalies[22].[23] The Feynman rules help us to investigate the Weyl anomaly in higher dimensional theories.
2. The graphical representation is taken at all stages. The familiar procedures in the ordinary perturbative treatment, such as the propagator rule and the vertex rule, are all graphically represented in coordinate space. The expanded terms themselves are also graphically represented. Especially we introduce "graphical calculation". This makes the higher-order calculation transparent and the Weyl anomaly calculation in the higher dimensions tractable.
3. We have not introduced any covariant quantities in intermediate stages. It is based on the weak-field perturbation. Although loosing manifest general covariance in intermediate stages, the expanded elements have the simplest symmetry (w.r.t. the suffix permutation) and are preferable for the computer algorithm.

4. We focus only on a special type of term: $(\partial\partial h)^n$, in the n dimensional space. These are the lowest order of the product of n Riemann tensors. We demonstrate they can determine the Weyl anomaly up to “trivial terms”.

In Sec.2 we briefly give the present formalism of the Weyl anomaly. The anomaly is given by the trace of the heat-kernel. In Sec.3 we present the Feynman rules to compute the heat-kernel *to any higher order*. They are naturally expressed in the *regularized* coordinate space, that is, the space of n -dim ordinary space-coordinates plus the proper time. As always in perturbative approaches, a graphical representation helps to systematically compute the heat-kernel at the higher order. The Taylor expansion, with respect to the “regularization” parameter t , is explained in Sec.4. The more the number of the space dimensions, the more expansion is necessary. We apply the general algorithm to the 6 dim scalar-gravity theory in Sec.5. We focus on four special graphs and introduce a new graphical calculation. The final result of the Weyl anomaly for the model is obtained in Sec.6. We conclude in Sec.7. Four appendices are provided to supplement the text. The propagator rules are given in App.A. Some supplementary calculation, relegated by Sec.5 of the text, is done in App.B. Weak field expansion of the 6 dim scalar-gravity is graphically given in App.C. The table of coefficients, when some general invariants are weak-field expanded, is given in App.D.

2 Formalism

Let us explain the present formulation of anomalies taking a simple example : n -dim Euclidean gravity-scalar coupled system. (see Ref.[22])

$$\begin{aligned} \mathcal{L}[g_{\mu\nu}, \phi] &= \sqrt{g}\phi\left(-\frac{1}{2}\nabla^2 + \frac{1}{2}qR\right)\phi \equiv \frac{1}{2}\tilde{\phi}\vec{D}\tilde{\phi} \quad , \\ q &= -\frac{n-2}{4(n-1)} \quad , \quad \vec{D}_x \equiv \sqrt[4]{g}\left(-\nabla_x^2 - \frac{n-2}{4(n-1)}R(x)\right)\frac{1}{\sqrt[4]{g}} \quad , \end{aligned} \quad (1)$$

where $g_{\mu\nu}$ and ϕ are the metric field and the scalar field respectively. We have introduced $\tilde{\phi} \equiv \sqrt[4]{g}\phi$ for the measure $\mathcal{D}\tilde{\phi}$ to be general coordinate (BRS) invariant [24]. This Lagrangian is invariant under the local Weyl transformation:

$$g^{\mu\nu}(x)' = e^{2\alpha(x)}g^{\mu\nu}(x) \quad , \quad \tilde{\phi}(x)' = e^{-\alpha(x)}\tilde{\phi}(x) \quad (\phi(x)' = e^{\frac{n-2}{2}\alpha(x)}\phi(x)) \quad , \quad (2)$$

where $\alpha(x)$ is the parameter of the local Weyl transformation.

Even if the Lagrangian is Weyl invariant, the quantum theory is generally not (Weyl anomaly). The effective action $\Gamma[g_{\mu\nu}]$ defined by

$$e^{-\Gamma[g_{\mu\nu}]} = \int \mathcal{D}\tilde{\phi} \exp\left\{-\int d^nx \mathcal{L}[g_{\mu\nu}, \phi]\right\} \quad , \quad (3)$$

changes as

$$\begin{aligned} e^{-\Gamma[g'_{\mu\nu}]} &= \int \mathcal{D}\tilde{\phi}' \exp\left\{-\int d^n x \mathcal{L}[g'_{\mu\nu}, \phi']\right\} \\ &= \int \mathcal{D}\tilde{\phi}(x) \det \frac{\partial \tilde{\phi}'(y)}{\partial \tilde{\phi}(x)} \exp\left\{-\int d^n x \mathcal{L}[g_{\mu\nu}, \phi]\right\} . \end{aligned} \quad (4)$$

The Weyl anomaly is given by the Jacobian[25, 26].

$$J \equiv \det \left[\frac{\partial \tilde{\phi}'(y)}{\partial \tilde{\phi}(x)} \right] = \exp\left(-\text{Tr} \alpha(x) \delta^n(x-y) + O(\alpha^2)\right) . \quad (5)$$

Taking the heat-kernel regularization, we obtain the expression for the Weyl anomaly as

$$\begin{aligned} J &= \exp\left(-\lim_{t \rightarrow +0} \text{Tr} [\alpha(x) G(x, y; t)] + O(\alpha^2)\right) , \\ \text{Weyl Anomaly} &= \left. \frac{\delta \Gamma}{\delta \alpha(x)} \right|_{\alpha=0} = -\left. \frac{\delta \ln J}{\delta \alpha(x)} \right|_{\alpha=0} = -2g^{\mu\nu} \langle T_{\mu\nu} \rangle = \lim_{t \rightarrow +0} \text{Tr} G(x, y; t) , \end{aligned} \quad (6)$$

where $G(x, y; t)$ is the heat-kernel defined by

$$\begin{aligned} \left(\frac{\partial}{\partial t} + \vec{D}_x \right) G(x, y; t) &= 0 , \quad G(x, y; t) \left(\frac{\overleftarrow{\partial}}{\partial t} + \vec{D}_y^\dagger \right) = 0 , \\ \lim_{t \rightarrow +0} G(x, y; t) &= \delta^n(x-y) . \end{aligned} \quad (7)$$

where \overleftarrow{D}_x means it operates on the left. The parameter t is regarded here as a regularization parameter and is called Schwinger's *proper time* [5]. The last equation expresses the regularization of the delta function $\delta^n(x-y)$ [27, 28]. $G(x, y; t)$ can be symbolically written as

$$G(x, y; t) \equiv \langle x | e^{-t\vec{D}} | y \rangle , \quad t > 0 . \quad (8)$$

We note here the physical dimension of the space coordinate x^μ and the proper-time t are

$$[x^\mu] = L , \quad [t] = L^2 , \quad (9)$$

where L is some length. For other (conformally invariant) theories, the Weyl anomaly is obtained by replacing the operator \vec{D} above. See ref.[22] for detail.

3 Feynman rules in coordinate space

3.1 Heat-kernel and Feynman graph

Let us solve Eq.(7) in weak-field perturbation theory. For a general theory with the derivative couplings up to the second order, the operator \vec{D}_x^{ij} can be always divided into the field-independent (free) part and the field-dependent (perturbation) one.

$$\begin{aligned}\vec{D}_x^{ij} &= -\delta_{\mu\nu}\delta^{ij}\partial_\mu\partial_\nu - \vec{V}^{ij}(x) \quad , \\ \vec{V}^{ij}(x) &\equiv W_{\mu\nu}^{ij}(x)\partial_\mu\partial_\nu + N_\mu^{ij}(x)\partial_\mu + M^{ij}(x) \quad , \\ i, j &= 1, 2, \dots, N \quad ,\end{aligned}\tag{10}$$

where $W_{\mu\nu}^{ij}$, N_μ^{ij} and M^{ij} are external fields (background coefficient fields) and the field suffixes (such as a fermion suffix and a vector suffix) i, j are introduced for the general use. In the present example (1), the above quantities are explicitly written as ($N = 1$)

$$\begin{aligned}\vec{V}(x) &= \sqrt[4]{g}(\nabla^\mu\nabla_\mu - qR)\frac{1}{\sqrt[4]{g}} - \delta_{\mu\nu}\partial_\mu\partial_\nu \quad , \\ W_{\mu\nu} &= g^{\mu\nu} - \delta_{\mu\nu} = -h_{\mu\nu} + h_{\mu\lambda}h_{\lambda\nu} + O(h^3) \quad , \\ N_\lambda &= -g^{\mu\nu}\Gamma_{\mu\nu}^\lambda - g^{\lambda\mu}\Gamma_{\mu\nu}^\nu = -\partial_\mu h_{\lambda\mu} + O(h^2) \quad , \\ M &= -qR + \frac{1}{4}g^{\mu\nu}\{\Gamma_{\mu\lambda}^\lambda\Gamma_{\nu\sigma}^\sigma + 2\Gamma_{\mu\nu}^\lambda\Gamma_{\lambda\sigma}^\sigma - 2\partial_\nu\Gamma_{\mu\lambda}^\lambda\} \\ &= -q(\partial^2 h - \partial_\alpha\partial_\beta h_{\alpha\beta}) - \frac{1}{4}\partial^2 h + O(h^2) \quad ,\end{aligned}\tag{11}$$

where $g_{\mu\nu} = \delta_{\mu\nu} + h_{\mu\nu}$, $h \equiv h_{\mu\mu}$. The graphical representation of $W_{\mu\nu}$, N_λ and M above is given, up to h^3 -order, for the $n=6$ dim case in App.C: Fig.16 for $W_{\mu\nu}$ and N_λ , Fig.17-21 for M . The usage of general coefficients $W_{\mu\nu}^{ij}$, N_μ^{ij} and M^{ij} , instead of their concrete contents, makes it possible to do the general treatment valid for many theories [22, 29, 30]. All equations below are valid for all theories so far as they have no higher-derivative interactions. Let us solve the differential equation (7) perturbatively for the case of weak external fields ($W_{\mu\nu}^{ij}$, N_μ^{ij} , M^{ij}). (In the present example, this corresponds to perturbation around *flat* space.) The differential equation (7) becomes

$$\begin{aligned}(\frac{\partial}{\partial t} - \partial^2)G^{ij}(x, y; t) &= \vec{V}^{ik}(x)G^{kj}(x, y; t) \quad , \\ \partial^2 &\equiv \delta_{\mu\nu}\partial_\mu\partial_\nu = \sum_{\mu=1}^n(\frac{\partial}{\partial x^\mu})^2 \quad .\end{aligned}\tag{12}$$

In the following we suppress the field suffixes i, j, \dots and take the matrix notation. This equation (12) is the n -dim heat equation with the small perturbation \vec{V} . We give two important quantities in order to obtain the solution. (This approach is popular in the perturbative quantum field theory under the name *propagator approach*[31]. In [31] the momentum representation is taken, which is to be compared with the coordinate one of the present approach. The Weyl anomaly in the string theory was analyzed in this approach by Alvarez[32].)

i) Heat Equation

The heat equation:

$$(\frac{\partial}{\partial t} - \partial^2)G_0(x, y; t) = 0 \quad , \quad t > 0 \quad (13)$$

has the solution

$$\begin{aligned} G_0(x, y; t) &= G_0(x - y; t) = \int \frac{d^n k}{(2\pi)^n} \exp\{-k^2 t + ik^\mu (x - y)^\mu\} I_N \\ &= \frac{1}{(4\pi t)^{n/2}} e^{-\frac{(x-y)^2}{4t}} I_N \quad , \quad k^2 \equiv \sum_{\mu=1}^n (k^\mu)^2 \quad , \end{aligned} \quad (14)$$

where I_N is the identity matrix of the size $N \times N$. G_0 satisfies the initial condition: $\lim_{t \rightarrow +0} G_0(x - y; t) = \delta^n(x - y) I_N$. We define

$$G_0(x, y; t) = 0 \text{ for } t \leq 0 \quad . \quad (15)$$

ii) Heat Propagator

The heat equation with the delta-function source defines the heat propagator.

$$\begin{aligned} (\frac{\partial}{\partial t} - \partial^2)S(x, y; t - s) &= \delta(t - s) \delta^n(x - y) I_N \quad , \\ S(x, y; t) &= S(x - y; t) = \int \frac{d^n k}{(2\pi)^n} \frac{dk^0}{2\pi} \frac{\exp\{-ik^0 t + ik \cdot (x - y)\}}{-ik^0 + k^2} I_N \\ &= \theta(t) G_0(x - y; t) \quad , \\ k^2 &\equiv \sum_{\mu=1}^n k^\mu k^\mu \quad , \quad k \cdot x \equiv \sum_{\mu=1}^n k^\mu x^\mu \quad . \end{aligned} \quad (16)$$

$\theta(t)$ is the *step function* defined by : $\theta(t) = 1$ for $t > 0$, $\theta(t) = 0$ for $t < 0$. $S(x - y; t)$ satisfies the initial condition: $\lim_{t \rightarrow +0} S(x - y; t) = \delta^n(x - y) I_N$ and $S(x, y; t) = 0$ for $t \leq 0$.

Now the formal solution of (12) with the initial condition (7) is given by

$$G(x, y; t) = G_0(x - y; t) + \int d^n z \int_{-\infty}^{\infty} ds S(x - z; t - s) \vec{V}(z) G(z, y; s) \quad . \quad (17)$$

$G(x, y; t)$ appears in both sides above. We can iteratively solve (17) as[5]

$$\begin{aligned} G(x, y; t) &= G_0(x - y; t) + \int S \vec{V} G_0 + \int S \vec{V} \int S \vec{V} G_0 + \cdots \quad , \\ G_1(x, y; t) &\equiv \int S \vec{V} G_0 = \int d^n z ds S(x - z; t - s) \vec{V}(z) G_0(z - y; s) \\ &= \int d^n z \int_0^t ds G_0(x - z; t - s) \vec{V}(z) G_0(z - y; s) \quad , \end{aligned} \quad (18)$$

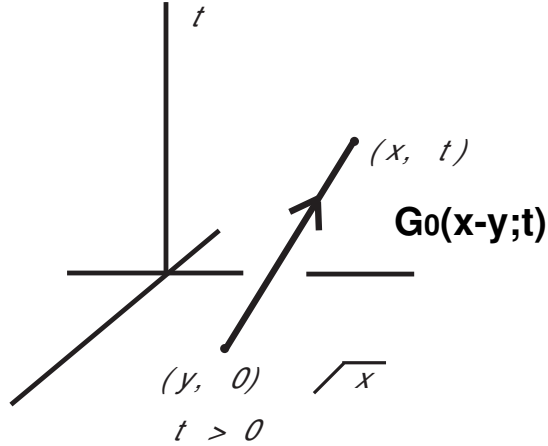


Fig.1 Graph of $G_0(x - y; t)$

$$\begin{aligned}
 G_2(x, y; t) &\equiv \int S \vec{V} \int S \vec{V} G_0 = \int d^n z' ds' S(x - z'; t - s') \vec{V}(z') \\
 &\quad \times \int d^n z ds S(z' - z; s' - s) \vec{V}(z) G_0(z - y; s) \\
 &= \int d^n z' \int_0^t ds' G_0(x - z'; t - s') \vec{V}(z') \\
 &\quad \times \int d^n z \int_0^{s'} ds G_0(z' - z; s' - s) \vec{V}(z) G_0(z - y; s) , \\
 G_3(x, y; t) &= \int d^n z'' \int_0^t ds'' G_0(x - z''; t - s'') \vec{V}(z'') \\
 &\quad \times \int d^n z' \int_0^{s''} ds' G_0(z'' - z'; s'' - s') \vec{V}(z') \\
 &\quad \times \int d^n z \int_0^{s'} ds G_0(z' - z; s' - s) \vec{V}(z) G_0(z - y; s) .
 \end{aligned}$$

Expressions for higher-order terms are similarly obtained.

As in the ordinary field theory, it is illuminating to represent this perturbative solution in graphs. We do it in the $(n+1)$ dimensional space, which is composed of the space of the ordinary n -dim (Euclidean) space plus 1-dim positive proper time. In the above solution, $G_0(x - y; t)$ plays the role of "propagator". It is represented by a directed[33] straight line as in Fig.1. $\vec{V}(z)$ plays the role of "vertex", which acts on the system, during the process of "propagation of particles", some times according to the perturbation order. The situation up to the 3-rd order is represented in Fig.2-4. We can easily write down the expression of any higher order, $G_k(x, y; t)$, with the help of this graphical representation.

Generally, in n -dim, the terms up to $G_{n/2}$ are sufficient for the anomaly calculation[22]. In this sense, the present expansion looks like that with respect to the space(-time) dimension.

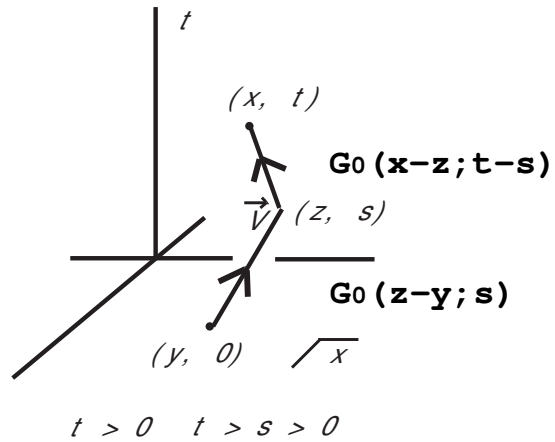


Fig.2 Graph of $G_1(x, y; t)$

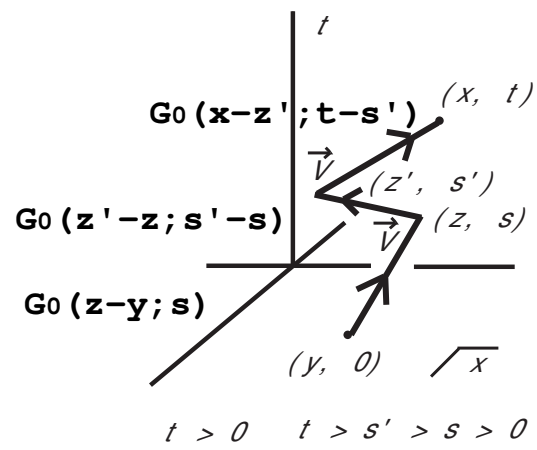


Fig.3 Graph of $G_2(x, y; t)$

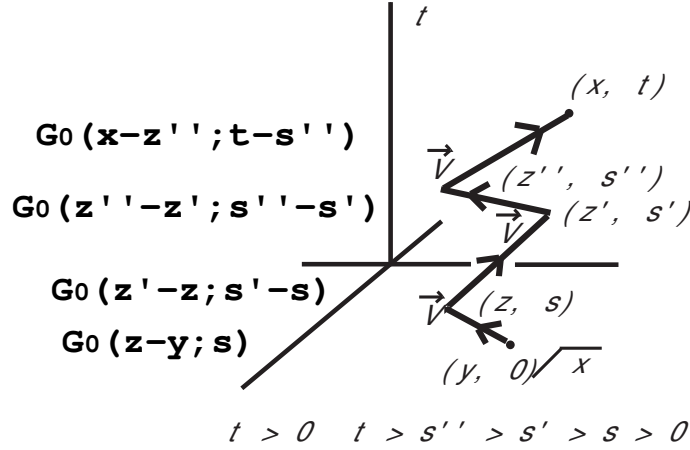


Fig.4 Graph of $G_3(x, y; t)$

3.2 Factoring out the scale parameter t

Because of the presence of the positive regularization parameter t , we can safely (without singularity) take the trace-part, $x = y$, in the above equations.

$$\begin{aligned} G(x, x; t) &= G_0(0; t) + G_1(x, x; t) + G_2(x, x; t) + G_3(x, x; t) + \dots, \\ G_0(0; t) &= \frac{1}{(4\pi t)^{n/2}} I_N. \end{aligned} \quad (19)$$

As shown in (6), the t^0 -part of $G(x, x; t)$ is the Weyl anomaly. In order to see their t -dependence, it is best to replace the dimensional coordinate variables such as (z, s) in (18) by the dimensionless ones (w, r) .

$$\begin{aligned} G_1(x, x; t) &\equiv \int S \vec{V} G_0 \Big|_{x=y} \\ &= \frac{1}{t^{(n/2)-1}} \int d^n w \int_0^1 dr G_0(w; 1-r) \vec{V}(x + \sqrt{t}w) G_0(w; r), \\ &1 > r = \frac{s}{t} > 0, \quad w = (z - x)/\sqrt{t}, \end{aligned} \quad (20)$$

$$(21)$$

where the relation (56) is used. In the same way, we obtain

$$\begin{aligned} G_2(x, x; t) &\equiv \int S \vec{V} \int S \vec{V} G_0 \Big|_{x=y} \\ &= \frac{1}{t^{(n/2)-2}} \int d^n w' \int_0^1 dr' G_0(w'; 1-r') \vec{V}(x + \sqrt{t}w') \\ &\quad \times \int d^n w \int_0^{r'} dr G_0(w' - w; r' - r) \vec{V}(x + \sqrt{t}w) G_0(w; r), \end{aligned} \quad (22)$$

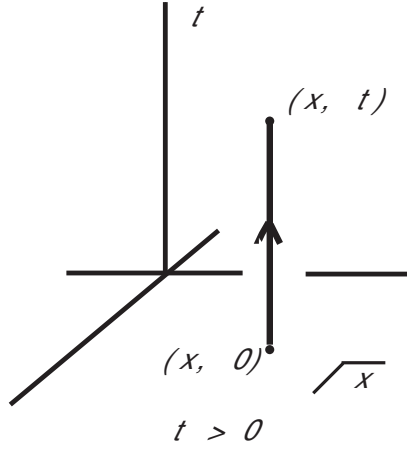


Fig.5 Graph of $G_0(0; t)$

where

$$\begin{aligned}
 1 &> r' = s'/t > r = s/t > 0, \quad w' = (z' - x)/\sqrt{t}, \quad w = (z - x)/\sqrt{t} \quad , \\
 G_3(x, x; t) &\equiv \int S\vec{V} \int S\vec{V} \int S\vec{V} G_0 \Big|_{x=y} \\
 &= \frac{1}{t^{(n/2)-3}} \int d^n w'' \int_0^1 dr'' G_0(w''; 1 - r'') \vec{V}(x + \sqrt{t}w'') \\
 &\quad \times \int d^n w' \int_0^{r''} dr' G_0(w'' - w'; r'' - r') \vec{V}(x + \sqrt{t}w') \\
 &\quad \times \int d^n w \int_0^{r'} dr G_0(w' - w; r' - r) \vec{V}(x + \sqrt{t}w) G_0(w; r) \quad , \tag{23}
 \end{aligned}$$

where

$$\begin{aligned}
 1 &> r'' = s''/t > r' = s'/t > r = s/t > 0, \\
 w'' &= (z'' - x)/\sqrt{t}, \quad w' = (z' - x)/\sqrt{t}, \quad w = (z - x)/\sqrt{t} \quad .
 \end{aligned}$$

The above quantities of $G_k(x, x; t)$, ($k = 0, \dots, 3$) are depicted in Fig.5-8 with the dimensionless quantities. We can easily write down higher-order terms with the help of graphs.

3.3 Vertex and propagator rules

The vertex operator $\vec{V}(x + \sqrt{t}w)$ in the expression $G_k(x, x; t)$ has differentials

$$\vec{V}(x + \sqrt{t}w) = \frac{1}{t} W_{\mu\nu}(x + \sqrt{t}w) \frac{\partial}{\partial w^\mu} \frac{\partial}{\partial w^\nu} + \frac{1}{\sqrt{t}} N_\mu(x + \sqrt{t}w) \frac{\partial}{\partial w^\mu} + M(x + \sqrt{t}w) \quad , \tag{24}$$

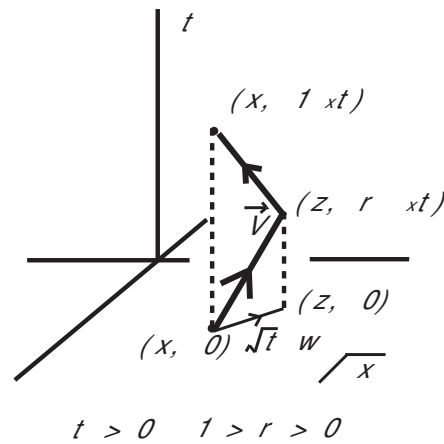


Fig.6 Graph of $G_1(x, x; t)$

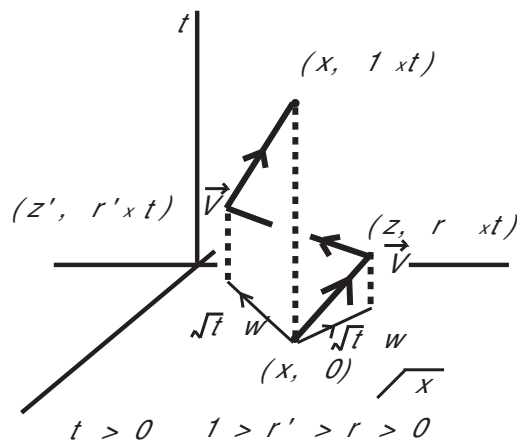


Fig.7 Graph of $G_2(x, x; t)$

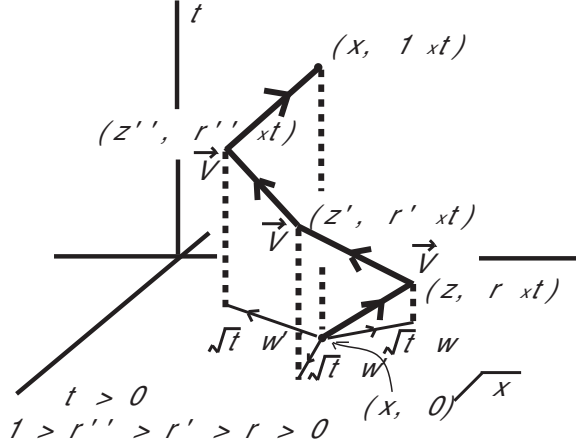


Fig.8 Graph of $G_3(x, x; t)$

and acts only on the "adjacently right" G_0 in Eqs.(20)-(23). Here we have the following *vertex rule*.

Vertex Rule 1

$$\begin{aligned}
 \vec{V}(x + \sqrt{t}w')G_0(w' - w; r' - r) &= \frac{1}{\{4\pi(r' - r)\}^{n/2}}\vec{V}(x + \sqrt{t}w')e^{-\frac{(w' - w)^2}{4(r' - r)}} \\
 &= \left\{ \frac{1}{t}W_{\mu\nu}(x + \sqrt{t}w') \left(-\frac{\delta_{\mu\nu}}{2(r' - r)} + \frac{(w' - w)_\mu(w' - w)_\nu}{4(r' - r)^2} \right) \right. \\
 &\quad \left. + \frac{1}{\sqrt{t}}N_\mu(x + \sqrt{t}w') \left(-\frac{(w' - w)_\mu}{2(r' - r)} \right) + M(x + \sqrt{t}w') \right\} G_0(w' - w; r' - r) \\
 &= V(x + \sqrt{t}w'; w' - w, r' - r; t)G_0(w' - w; r' - r) \quad ,
 \end{aligned}$$

where

$$V(x; w, r; t) \equiv \frac{1}{t}W_{\mu\nu}(x) \left(-\frac{\delta_{\mu\nu}}{2r} + \frac{w_\mu w_\nu}{4r^2} \right) + \frac{1}{\sqrt{t}}N_\mu(x) \left(-\frac{w_\mu}{2r} \right) + M(x) \quad , \quad (25)$$

where V does *not* have differentials. Especially taking $r = 0, w = 0$ in the above and dropping primes ('), we obtain a relation.

Vertex Rule 2

$$\begin{aligned}
 \vec{V}(x + \sqrt{t}w)G_0(w; r) &= \left\{ \frac{1}{t}W_{\mu\nu}(x + \sqrt{t}w) \left(-\frac{\delta_{\mu\nu}}{2r} + \frac{w_\mu w_\nu}{4r^2} \right) + \frac{1}{\sqrt{t}}N_\mu(x + \sqrt{t}w) \left(-\frac{w_\mu}{2r} \right) + M(x + \sqrt{t}w) \right\} G_0(w; r) \\
 &= V(x + \sqrt{t}w; w, r; t)G_0(w; r) \quad .
 \end{aligned} \quad (26)$$

Making use of the above rule, we can evaluate $G_1(x, x; t)$ of Eq.(20) as

$$\begin{aligned}
 G_1(x, x; t) &= \frac{1}{t^{(n/2)-1}} \int d^n w \int_0^1 dr G_0(w; 1 - r)G_0(w; r)V(x + \sqrt{t}w; w, r; t) \\
 &= \frac{1}{(4\pi)^{n/2}t^{(n/2)-1}} \int d^n w \int_0^1 dr G_0(w; (1 - r)r)V(x + \sqrt{t}w; w, r; t) \quad ,
 \end{aligned} \quad (27)$$

where the relation: $G_0(w; 1 - k)G_0(w; r) = \frac{1}{(4\pi)^{n/2}}G_0(w; (1 - r)r)$, $1 > r > 0$, which is derived from a *propagator rule 4* (62), is used in order to reduce the number of G_0 's by one. In Appendix A, we list the propagator rules (59-62), and their graphical ("geometrical") expressions in the coordinate space: Fig.10-13. $G_2(x, x; t)$ of Eq.(22) is written, in terms of V , as

$$G_2(x, x; t) = \frac{1}{t^{(n/2)-2}} \int d^n w' \int_0^1 dr' G_0(w'; 1 - r') \times \int d^n w \int_0^{r'} dr V(x + \sqrt{t}w'; w' - w, r' - r; t) G_0(w' - w; r' - r) V(x + \sqrt{t}w; w, r; t) G_0(w; r) \quad .(28)$$

By changing the integration variable w' to a new one \bar{w} defined below, we can make all G_0 's have space-variables independent of each other. Using the following relations,

$$G_0(w'; 1 - r')G_0(w' - w; r' - r) = G_0(\bar{w}; \frac{(1 - r')(r' - r)}{1 - r})G_0(w; 1 - r) \quad ,$$

$$1 > r' > r \quad , \bar{w} = w' - \frac{1 - r'}{1 - r}w \quad ,$$

$$G_0(w; 1 - r)G_0(w; r) = \frac{1}{(4\pi)^{n/2}}G_0(w; (1 - r)r) \quad , \quad 1 > r > 0 \quad , \quad (29)$$

which are obtained from Rule 2 ,(60), and Rule 3 ,(62), respectively, we can finally evaluate eq.(28) as

$$G_2(x, x; t) = \frac{1}{(4\pi)^{n/2}t^{(n/2)-2}} \int d^n \bar{w} \int_0^1 dr' \int d^n w \int_0^{r'} dr \times G_0(\bar{w}; \frac{(1 - r')(r' - r)}{1 - r})G_0(w; (1 - r)r) V(x + \sqrt{t}w'; w' - w, r' - r; t) V(x + \sqrt{t}w; w, r; t) \quad ,$$

$$w' = \bar{w} + \frac{1 - r'}{1 - r}w \quad , \quad (30)$$

where the integration variable w' is changed to \bar{w} ($\det \frac{\partial(w', w)}{\partial(\bar{w}, w)} = 1$). We note the following things in the above evaluation.

1. The number of propagators , G_0 's, decreases by one and becomes the same as that of the space integration variables.
2. All "Gaussian" coordinates in G_0 's (\bar{w} and w in the present case) can be taken independent
3. In the above reduction, we have applied the propagator rules on G_0 's from "left" to "right". There are some other choices (for example, from "right" to "left") which give expressions different from (30) in appearance.

These properties are valid for any order of $G_k(x, x; t)$.

Similarly we can evaluate G_3 as

$$\begin{aligned}
G_3(x, x; t) &= \frac{1}{(4\pi)^{n/2} t^{(n/2)-3}} \int d^n \bar{w} \int d^n \bar{w} \int d^n w \int_0^1 dr'' \int_0^{r''} dr' \int_0^{r'} dr \\
&\times G_0(\bar{w}; \frac{(1-r'')(r''-r')}{1-r'}) G_0(\bar{w}; \frac{(1-r')(r'-r)}{1-r}) G_0(w; (1-r)r) \\
&\times V(x + \sqrt{t}w''; w'' - w', r'' - r'; t) V(x + \sqrt{t}w'; w' - w, r' - r; t) V(x + \sqrt{t}w; w, r; t) , \\
w'' &= \bar{w} + \frac{1-r''}{1-r'} \bar{w} + \frac{1-r''}{1-r} w , w' = \bar{w} + \frac{1-r'}{1-r} w , \quad (31)
\end{aligned}$$

where the integration variables w'' and w' are changed to \bar{w} and \bar{w} ($\det \frac{\partial(w'', w', w)}{\partial(\bar{w}, \bar{w}, w)} = 1$). As in G_2 , there are some different expressions depending on how we apply the propagator rules in G_0 's.

Because of the integration formulae (57) of App.A, the space integrations in (27),(30) and (31) give a product of Kronecker's deltas times some rational function of dimensionless parameters. From above results we can write down $G_k(x, x; t)$ for any higher k . $G_k(x, x; t)$ has k -fold parameter integrals.

4 Evaluation of t^0 -Part of $G(x, x; t)$

— Taylor expansion for taking the limit $t \rightarrow +0$ —

Let us evaluate $G(x, x; t)|_{t^0}$. We consider $n = 6$ dim space. We focus on the $(\partial\partial h)^3$ -type terms, because that part has the sufficient information to determine the Weyl anomaly in 6 dim. Taking the Taylor-expansion of $W_{\mu\nu}(x + \sqrt{t}v)$, $N_\mu(x + \sqrt{t}v)$ and $M(x + \sqrt{t}v)$ around $\sqrt{t}v = 0$, $V(x + \sqrt{t}v; w, r; t)$ can be expanded as

$$\begin{aligned}
V(x + \sqrt{t}v; w, r; t) &= \frac{1}{t} W_{\mu\nu}(x + \sqrt{t}v) \left(-\frac{\delta_{\mu\nu}}{2r} + \frac{w_\mu w_\nu}{4r^2} \right) + \frac{1}{\sqrt{t}} N_\mu(x + \sqrt{t}v) \left(-\frac{w_\mu}{2r} \right) + M(x + \sqrt{t}v) \\
&= \frac{1}{t} V_{-1}(x, v; w, r) + V_0('') + t V_1('') + \cdots + \frac{1}{\sqrt{t}} V_{-1/2}('') + \sqrt{t} V_{1/2}('') + \cdots , \quad (32)
\end{aligned}$$

where $V_{-1/2}, V_{1/2}, \dots$ are irrelevant parts because they all have odd-time derivatives of h 's: $\partial h, \partial\partial\partial h, \dots$. $V_{-1}('') = W_{\mu\nu}(x) \left(-\frac{\delta_{\mu\nu}}{2r} + \frac{w_\mu w_\nu}{4r^2} \right)$ is also irrelevant because it has no derivatives of h 's.[34] V_0, V_1, V_2 are given by

$$\begin{aligned}
V_0(x, v; w, r) &= \frac{1}{2!} \partial_{\alpha_1} \partial_{\alpha_2} W_{\mu\nu} \cdot v^{\alpha_1} v^{\alpha_2} \left(-\frac{\delta_{\mu\nu}}{2r} + \frac{w_\mu w_\nu}{4r^2} \right) + \partial_{\alpha_1} N_\mu \cdot v^{\alpha_1} \left(-\frac{w_\mu}{2r} \right) + M , \\
V_1(x, v; w, r) &= \frac{1}{4!} \partial_{\alpha_1} \partial_{\alpha_2} \cdots \partial_{\alpha_4} W_{\mu\nu} \cdot v^{\alpha_1} v^{\alpha_2} \cdots v^{\alpha_4} \left(-\frac{\delta_{\mu\nu}}{2r} + \frac{w_\mu w_\nu}{4r^2} \right) \\
&+ \frac{1}{3!} \partial_{\alpha_1} \partial_{\alpha_2} \partial_{\alpha_3} N_\mu \cdot v^{\alpha_1} v^{\alpha_2} v^{\alpha_3} \left(-\frac{w_\mu}{2r} \right) + \frac{1}{2!} \partial_{\alpha_1} \partial_{\alpha_2} M \cdot v^{\alpha_1} v^{\alpha_2} , \\
V_2(x, v; w, r) &= \frac{1}{6!} \partial_{\alpha_1} \partial_{\alpha_2} \cdots \partial_{\alpha_6} W_{\mu\nu} \cdot v^{\alpha_1} v^{\alpha_2} \cdots v^{\alpha_6} \left(-\frac{\delta_{\mu\nu}}{2r} + \frac{w_\mu w_\nu}{4r^2} \right) \\
&+ \frac{1}{5!} \partial_{\alpha_1} \partial_{\alpha_2} \cdots \partial_{\alpha_5} N_\mu \cdot v^{\alpha_1} v^{\alpha_2} \cdots v^{\alpha_5} \left(-\frac{w_\mu}{2r} \right) \\
&+ \frac{1}{4!} \partial_{\alpha_1} \partial_{\alpha_2} \cdots \partial_{\alpha_4} M \cdot v^{\alpha_1} v^{\alpha_2} \cdots v^{\alpha_4} . \quad (33)
\end{aligned}$$

The Taylor-expansion of $W_{\mu\nu}, N_\mu, M$, for the case of the 6 dim scalar-gravity theory, is graphically shown in App.C: (72) for V_0 , (74) for V_1 and (76) for V_2 .

Now we pick up the t^0 -part[35] and focus on the $(\partial\partial h)^3$ -terms in the final form. For $G_1(x, x; t)$

$$G_1(x, x; t) = \frac{1}{(4\pi)^3} \int_0^1 dr \int d^6 w G_0(w; (1-r)r) \left[\frac{1}{t^2} V(x + \sqrt{t}w; w, r; t) \right] ,$$

$$\left[\frac{1}{t^2} V'' \right] |_{t^0} = V_2(x, w; w, r) . \quad (34)$$

We notice the $w^{\alpha_1} w^{\alpha_2} \dots$ parts give , after the w -integration, different products of Kronecker's deltas times powers of $(1-r)r$. See (57).

As for $G_2(x, x; t)$, from (30),

$$G_2(x, x; t) = \frac{1}{(4\pi)^3} \int_0^1 dr' \int_0^{r'} dr \int d^6 \bar{w} \int d^6 w$$

$$\times G_0(\bar{w}; \frac{(1-r')(r'-r)}{1-r}) G_0(w; (1-r)r) \left[\frac{1}{t} V(x + \sqrt{t}w'; w' - w, r' - r; t) V(x + \sqrt{t}w; w, r; t) \right] ,$$

$$\left[\frac{1}{t} V'' V''' \right] |_{t^0} = V_1(x, w'; w' - w, r' - r) V_0(x, w; w, r) + V_0(x, w'; w' - w, r' - r) V_1(x, w; w, r)$$

$$+ \text{irrel. terms} ,$$

$$w' = \bar{w} + R_1 w , \quad w' - w = \bar{w} - S_1 w ,$$

$$R_1 \equiv \frac{1-r'}{1-r} \equiv R(r, r') , \quad S_1 \equiv \frac{r'-r}{1-r} \equiv S(r, r') , \quad R_1 > 0 , \quad S_1 > 0 , \quad R_1 + S_1 = 1 . \quad (35)$$

The functions $R(r, r')$ and $S(r, r')$ will be used in (37). The irrelevant terms ("irrel. terms") are such ones as $V_2 V_{-1}$, $V_{1/2} V_{1/2}$, etc.

As for $G_3(x, x; t)$, from (31),

$$G_3(x, x; t) = \frac{1}{(4\pi)^3} \int_0^1 dr'' \int_0^{r''} dr' \int_0^{r'} dr \int d^6 \bar{w} \int d^6 \bar{w} \int d^6 w$$

$$\times G_0(\bar{w}; \frac{(1-r'')(r'' - r')}{1-r'}) G_0(\bar{w}; \frac{(1-r')(r' - r)}{1-r}) G_0(w; (1-r)r)$$

$$\times \left[V(x + \sqrt{t}w''; w'' - w', r'' - r'; t) V(x + \sqrt{t}w'; w' - w, r' - r; t) V(x + \sqrt{t}w; w, r; t) \right] ,$$

$$[V'' V''' V'''']|_{t^0} = V_0(x, w''; w'' - w', r'' - r') V_0(x, w'; w' - w, r' - r) V_0(x, w; w, r)$$

$$+ \text{irrel. terms} , \quad (36)$$

where "irrel. terms" above are such ones as $V_1 V_{-1} V_0$, $V_{1/2} V_{1/2} V_0$, etc. In the above, the coordinate variables in the integrand are written by the integration variables \bar{w}, \bar{w} and w as

$$w'' = \bar{w} + R_2 \bar{w} + R_3 w , \quad w'' - w' = \bar{w} - S_2 \bar{w} - T_1 w ,$$

$$w' = \bar{w} + R_1 w , \quad w' - w = \bar{w} - S_1 w ,$$

$$\text{where}$$

$$\begin{aligned}
R_1 &= R(r, r') = \frac{1-r'}{1-r} \quad , \quad R_2 = R(r', r'') = \frac{1-r''}{1-r'} \quad , \quad R_3 = R(r, r'') = \frac{1-r''}{1-r} \quad , \\
S_1 &= S(r, r') = \frac{r'-r}{1-r} \quad , \quad S_2 = S(r', r'') = \frac{r''-r'}{1-r'} \quad , \quad T_1 = \frac{r''-r'}{1-r} \equiv T(r, r', r'') \quad ,
\end{aligned} \tag{37}$$

where $R(r, r')$ and $S(r, r')$ was introduced in the previous order (35), and $T(r, r', r'')$ is a new function. R_i, S_i and T_1 have the following relations.

$$\begin{aligned}
R_1 + S_1 &= 1 \quad , \quad R_2 + S_2 = 1 \quad , \quad R_3 + T_1 = R_1 \quad , \quad \frac{R_3}{R_2} = R_1 \quad , \quad \frac{T_1}{S_2} = R_1 \quad , \\
R_1, R_2, R_3, S_1, S_2, T_1 &> 0 \quad .
\end{aligned} \tag{38}$$

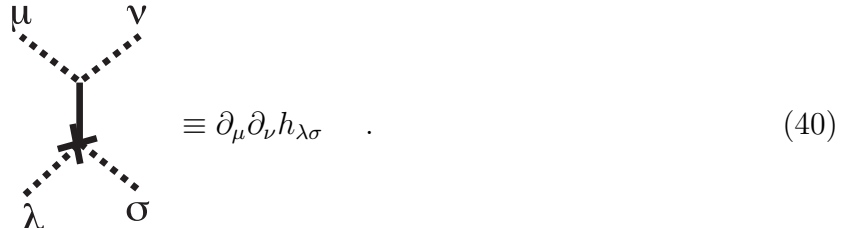
Here we finish treating the Weyl anomaly $G(x, x; t)|_{t=0}$ in terms of the general ones: $(W_{\mu\nu}, N_\lambda, M)$ and their derivatives. Their explicit forms depend on each model. The content of App.C comes from the 6 dim scalar-gravity theory (11). In the following two sections, we explain how we obtain the explicit form of the Weyl anomaly using the obtained formulae .

5 Four Special Graphs

In the 6 dim space, there are four “important general invariants” as the Weyl anomaly terms, which will be explained in the next section. In order to obtain the four coefficients of those terms, let us determine the coefficients of the following four $(\partial\partial h)^3$ -terms which appear in $G(x, x; t)|_{t=0}$.

$$\begin{aligned}
\text{Graph3} &= \partial_\sigma \partial_\tau h_{\mu\nu} \cdot \partial_\nu \partial_\lambda h_{\tau\omega} \cdot \partial_\omega \partial_\mu h_{\lambda\sigma} \quad , \\
\text{Graph67} &= \partial_\tau \partial_\omega h_{\mu\nu} \cdot \partial_\mu \partial_\nu h_{\lambda\sigma} \cdot \partial_\lambda \partial_\sigma h_{\tau\omega} \quad , \\
\text{Graph1} &= \partial_\mu \partial_\nu h_{\nu\lambda} \cdot \partial_\lambda \partial_\sigma h_{\sigma\tau} \cdot \partial_\tau \partial_\omega h_{\omega\mu} \quad , \\
\text{Graph2} &= \partial_\mu \partial_\nu h_{\tau\sigma} \cdot \partial_\sigma \partial_\lambda h_{\lambda\nu} \cdot \partial_\tau \partial_\omega h_{\omega\mu} \quad .
\end{aligned} \tag{39}$$

Here we introduce a useful graphical representation to express $\text{SO}(n)$ invariants like given above. (See ref.[46] for detail.) We graphically express the basic ingredient $\partial_\mu \partial_\nu h_{\lambda\sigma}$ as



The contraction of suffixes is expressed by gluing the corresponding suffix-lines. Then the above four terms (39) are graphically shown in Fig.9. The advantage of this representation is that the way suffixes are contracted can be read by the topology of the graph. We need not

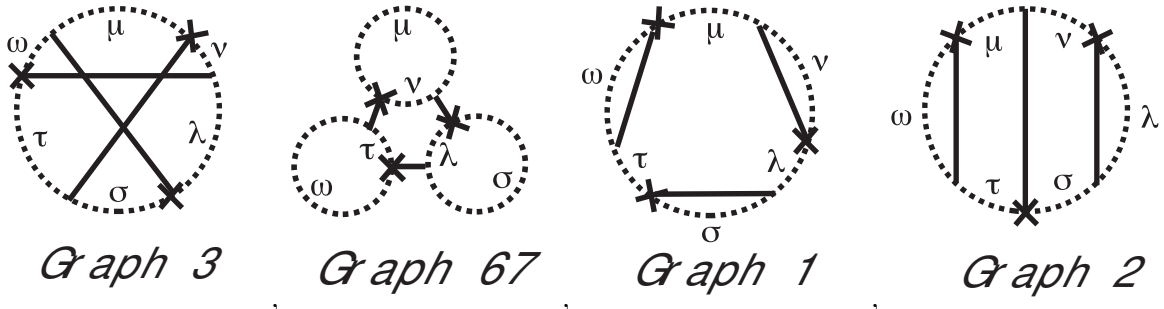


Fig.9 Four Graphs of 3,67,1 and 2. See the (40) for the definition of the graph.

bother about the dummy contracted suffixes. For later use, we introduce the following usage too.

$$\equiv \partial_\mu \partial_\nu h_{\lambda\sigma} \cdot v^\mu v^\nu , \quad \equiv \partial_\mu \partial_\nu h_{\lambda\sigma} \cdot v^\mu v^\nu w^\lambda w^\sigma . \quad (41)$$

The choice of those graphs (39) is an important step of this algorithm. As will be explained in Sec.6, it is done by looking the table of App.D and the content of the “important invariants”. In the evaluation, we exploit the topology of graphs in order to efficiently select relevant terms. All four graphs above come only from $G_3(x, x; t)|_{t^0}$. It is graphically seen by the following common features:

- There is no .
- No tadpoles (,) .

and the structure of G_1 and G_2 :

$$G_1(x, x; t)|_{t^0} \sim \int dr \int d^6 w G_0(w; (1-r)r) V_2(x, w; w, r) ,$$

$$G_2(x, x; t)|_{t^0} \sim \int dr' \int dr \int d^6 \bar{w} \int d^6 w G_0(\bar{w}; \frac{(1-r')(r'-r)}{1-r}) G_0(w; (1-r)r) \{ V_1(x, w'; w' - w, r' - r) V_0(x, w; w, r) + V_0(x, w'; w' - w, r' - r) V_1(x, w; w, r) \} , \quad (42)$$

where V_2 , V_1 and V_0 are graphically shown in App.C.2. Both $G_1|_{t=0}$ and $G_2|_{t=0}$ contain, at least, one of two graph-ingredients itemized above. For simplicity we focus, in this section, only on Graphs 3 and 67. Graph 1 and 2 are evaluated in App.B. Because of the following common features of Graph 3 and 67,

- No tadpoles.

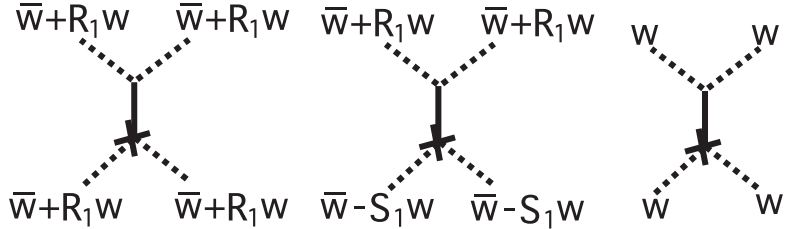
- There is no .

we can reduce the expression of $G_3(x, x; t)|_{t^0}$, (36) with V_0 given by (71) and (72), to the following form as the relevant part.

$$G_3(x, x; t)|_{t^0} = \frac{1}{(4\pi)^3} \int_0^1 dr'' \int_0^{r''} dr' \int_0^{r'} dr \int d^6 \bar{w} \int d^6 \bar{w} \int d^6 w$$

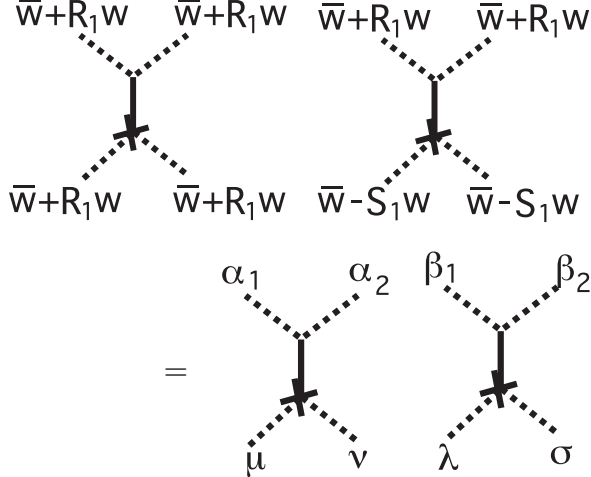
$$\times G_0(\bar{w}; \frac{(1-r'')(r''-r')}{1-r'}) G_0(\bar{w}; \frac{(1-r')(r'-r)}{1-r}) G_0(w; (1-r)r)$$

$$\times (-\frac{1}{2})^3 \times \frac{1}{4(r''-r')^2} \times \frac{1}{4(r'-r)^2} \times \frac{1}{4r^2} \times (R_2)^2 (S_2)^2 \times$$



+irrelevant terms , (43)

where the relations $\frac{R_3}{R_2} = R_1$, $\frac{T_1}{S_2} = R_1$ are used (see (38)). Furthermore, again by the common features of the graphs 3 and 67, we see no contribution comes from \bar{w}^8 - and \bar{w}^6 -terms.[36]



$$\times \{(R_1)^6 (S_1)^2 w^{\alpha_1} w^{\alpha_2} w^\mu w^\nu w^{\beta_1} w^{\beta_2} w^\lambda w^\sigma$$

$$+ (R_1)^6 w^{\alpha_1} w^{\alpha_2} w^\mu w^\nu w^{\beta_1} w^{\beta_2} \bar{w}^\lambda \bar{w}^\sigma$$

$$- (R_1)^5 S_1 (w^{\alpha_1} w^{\alpha_2} w^\mu w^\nu w^{\beta_1} \bar{w}^{\beta_2} + {}_6 C_1) \bar{w}^\lambda w^\sigma \times 2$$

$$+ (R_1)^4 (S_1)^2 (w^{\alpha_1} w^{\alpha_2} w^\mu w^\nu \bar{w}^{\beta_1} \bar{w}^{\beta_2} + {}_6 C_2) w^\lambda w^\sigma$$

$$+ (R_1)^2 (S_1)^2 (\bar{w}^{\alpha_1} \bar{w}^{\alpha_2} \bar{w}^\mu \bar{w}^\nu w^{\beta_1} w^{\beta_2} + {}_6 C_4) w^\lambda w^\sigma$$

$$\begin{aligned}
& - (R_1)^3 (S_1) (\bar{w}^{\alpha_1} \bar{w}^{\alpha_2} \bar{w}^\mu w^\nu w^{\beta_1} w^{\beta_2} + {}_6 C_3) \bar{w}^\lambda w^\sigma \times 2 \\
& + (R_1)^4 (\bar{w}^{\alpha_1} \bar{w}^{\alpha_2} w^\mu w^\nu w^{\beta_1} w^{\beta_2} + {}_6 C_2) \bar{w}^\lambda \bar{w}^\sigma \} \\
& + O(\bar{w}^6) + O(\bar{w}^8) , \tag{44}
\end{aligned}$$

where ${}_m C_r$ means "other choices of r \bar{w} 's among m suffixes appearing in the first term within the brackets". The \bar{w}, \bar{w}, w -integrations are three independent Gaussian integrations, and they give the product of two parts for each term. One part is a rational function of the parameters and the other is a symmetrized product of the Kronecker's deltas. In terms of a "components" notation:

$$\langle c_1, c_2 \rangle \equiv c_1(\text{Graph3}) + c_2(\text{Graph67}) , \tag{45}$$

the final result is evaluated as

$$\begin{aligned}
G_3(x, x; t)|_{t^0} &= \frac{1}{(4\pi)^3} \int_0^1 dr'' \int_0^{r''} dr' \int_0^{r'} dr \times \left(-\frac{1}{2}\right)^3 \times \frac{1}{4(r'' - r')^2} \times \frac{1}{4(r' - r)^2} \times \frac{1}{4r^2} \\
&\quad \times (R_2)^2 (S_2)^2 \times \left[(R_1)^6 (S_1)^2 \{2(1-r)r\}^6 \times \langle 64, 16 \rangle \right. \\
&\quad + 2 \frac{(1-r')(r'-r)}{1-r} \{2(1-r)r\}^5 \times \{(R_1)^6 \langle 0, 0 \rangle - 2(R_1)^5 S_1 \langle 32, 8 \rangle \right. \\
&\quad \quad \quad \left. \left. + (R_1)^4 (S_1)^2 \langle 64, 16 \rangle \right\} \right. \\
&\quad + \left\{ 2 \frac{(1-r')(r'-r)}{1-r} \right\}^2 \{2(1-r)r\}^4 \times \{(R_1)^2 (S_1)^2 \langle 0, 8 \rangle - 2(R_1)^3 S_1 \langle 32, 0 \rangle \right. \\
&\quad \quad \quad \left. \left. + (R_1)^4 \langle 0, 8 \rangle \right\} \right] \\
&\quad + \text{other graph-terms} \\
&= \frac{1}{(4\pi)^3} \left\langle \frac{4}{27 \times 105}, -\frac{1}{36 \times 63} \right\rangle + \text{other graph-terms} . \tag{46}
\end{aligned}$$

The above numbers $\langle c_1, c_2 \rangle$ are obtained by a computer calculation[37]. The numbers c_1 and c_2 show the "weights" when a symmetrized product of Kronecker's deltas are multiplied to a $(\partial \partial h)^3$ -tensor. For example the first one of (46), $\langle 64, 16 \rangle$, says

$$\begin{aligned}
& \text{Diagram: } \begin{array}{c} \alpha_1 \quad \alpha_2 \quad \beta_1 \quad \beta_2 \quad \gamma_1 \quad \gamma_2 \\ \text{---} \quad \text{---} \quad \text{---} \quad \text{---} \quad \text{---} \quad \text{---} \\ | \quad | \quad | \quad | \quad | \quad | \\ u \quad v \quad \lambda \quad \sigma \quad \tau \quad \omega \end{array} \times [\alpha_1 \alpha_2 \mu \nu \beta_1 \beta_2 \lambda \sigma \gamma_1 \gamma_2 \tau \omega] \\
& = 64(\text{Graph3}) + 16(\text{Graph67}) + \text{other graph-terms} , \tag{47}
\end{aligned}$$

where the notation $[\alpha_1 \alpha_2 \dots]$ is the symmetrized product of Kronecker's deltas and is defined in (58) of App.A. Note that in the expression just before the parameter integral, poles at $r = 1$, $r' = 1$ cancel out and there remain no divergences of the parameter integrals. This

occurs also in the calculation in App.B. Adding the result for Graph1 and 2 explained in App.B, we obtain finally the total contribution of $G(x, x; t)|_{t^0}$ to the four graphs as

$$G(x, x; t)|_{t^0} = \frac{1}{(4\pi)^3} \left\{ \frac{4}{27 \times 105} (\text{Graph3}) - \frac{1}{36 \times 63} (\text{Graph67}) + \frac{1}{36 \times 630} (\text{Graph1}) \right. \\ \left. + \frac{1}{36 \times 35} (\text{Graph2}) \right\} + \text{other terms} \quad . \quad (48)$$

6 Final Invariant Form of 6 Dim Weyl Anomaly

The general structure of the Weyl anomaly has been analyzed by refs.[38, 39, 40]. They claim that the Weyl anomaly is composed of three types of term: A) the Euler term; B) Conformal invariants; C) Trivial terms. Trivial terms are those which can be absorbed by local counter-terms made of the metric. This statement is checked by the cohomology analysis up to 6 dimensions[2]. We called, in Sec.5, the A and B terms “important invariants”. Therefore we may write, for the present 6 dim case,

$$G(x, x; t)|_{t^0} = \frac{1}{(4\pi)^3} \sqrt{g} \{ xC_1 + yC_2 + zC_3 + wE + \text{trivial terms} \} \\ C_1 = C_{\mu\nu\lambda\sigma} C^{\sigma\lambda\alpha\beta} C_{\beta\alpha}^{\nu\mu} , \quad C_2 = C_{\mu\nu\alpha\sigma} C^{\nu\lambda\beta\alpha} C_{\lambda\beta}^{\mu\sigma} , \\ C_3 \sim C_{\mu\nu\alpha\beta} \nabla^2 C^{\mu\nu\alpha\beta} + \dots , \quad E \sim R_{\mu\nu\alpha\beta} R_{\lambda\sigma\gamma\delta} R_{\tau\omega\epsilon\theta} \epsilon^{\mu\nu\lambda\sigma\tau\omega} \epsilon^{\alpha\beta\gamma\delta\epsilon\theta} , \\ C_{\mu\nu\sigma}^{\lambda} = R_{\mu\nu\sigma}^{\lambda} + \frac{1}{4} (\delta_{\nu}^{\lambda} R_{\mu\sigma} + g_{\mu\sigma} R_{\nu}^{\lambda} - \nu \leftrightarrow \sigma) + \frac{1}{20} (\delta_{\sigma}^{\lambda} g_{\mu\nu} - \nu \leftrightarrow \sigma) R , \quad (49)$$

where $C_{\mu\nu\sigma}^{\lambda}$ is the Weyl tensor, C_1, C_2 and C_3 are three independent conformal invariants, and E is the Euler term. x, y, z , and w are some constants to be determined. It is well-established that all possible independent invariants (parity even) with mass-dimension 6 are, in the 6 and higher space-dimensions, given by the following 17 terms[2, 41, 42].

$$P_1 = RRR , \quad P_2 = RR_{\mu\nu} R^{\mu\nu} , \quad P_3 = RR_{\mu\nu\lambda\sigma} R^{\mu\nu\lambda\sigma} , \\ P_4 = R_{\mu\nu} R^{\nu\lambda} R_{\lambda}^{\mu} , \quad P_5 = -R_{\mu\nu\lambda\sigma} R^{\mu\lambda} R^{\nu\sigma} , \quad P_6 = R_{\mu\nu\lambda\sigma} R_{\tau}^{\nu\lambda\sigma} R^{\mu\tau} , \\ A_1 = R_{\mu\nu\lambda\sigma} R^{\sigma\lambda}_{\tau\omega} R^{\omega\tau\nu\mu} , \quad B_1 = R_{\mu\nu\tau\sigma} R^{\nu}_{\lambda\omega} R^{\lambda\mu\sigma\omega} , \\ O_1 = \nabla^{\mu} R \cdot \nabla_{\mu} R , \quad O_2 = \nabla^{\mu} R_{\lambda\sigma} \cdot \nabla_{\mu} R^{\lambda\sigma} , \\ O_3 = \nabla^{\mu} R^{\lambda\rho\sigma\tau} \cdot \nabla_{\mu} R_{\lambda\rho\sigma\tau} , \quad O_4 = \nabla^{\mu} R_{\lambda\nu} \cdot \nabla^{\nu} R^{\lambda}_{\mu} , \\ T_1 = \nabla^2 R \cdot R , \quad T_2 = \nabla^2 R_{\lambda\sigma} \cdot R^{\lambda\sigma} , \quad T_3 = \nabla^2 R_{\lambda\rho\sigma\tau} \cdot R^{\lambda\rho\sigma\tau} , \\ T_4 = \nabla^{\mu} \nabla^{\nu} R \cdot R_{\mu\nu} , \\ S = \nabla^2 \nabla^2 R . \quad (50)$$

In terms of above 17 ”basis”, we can rewrite (49) as follows.

$$C_1 = \frac{9}{200} P_1 - \frac{27}{40} P_2 + \frac{3}{10} P_3 + \frac{5}{4} P_4 + \frac{3}{2} P_5 - 3P_6 + A_1 ,$$

$$\begin{aligned}
C_2 &= -\frac{19}{800}P_1 + \frac{57}{160}P_2 - \frac{3}{40}P_3 - \frac{7}{16}P_4 - \frac{9}{8}P_5 + \frac{3}{4}P_6 + B_1 \quad , \\
C_3 &= P_1 - 8P_2 - 2P_3 + 10P_4 + 10P_5 - \frac{1}{2}T_1 + 5T_2 - 5T_3 \quad , \\
E &= P_1 - 12P_2 + 3P_3 + 16P_4 + 24P_5 - 24P_6 + 4A_1 - 8B_1 \quad , \\
G(x, x; t)|_{t^0} &= \frac{1}{(4\pi)^3} \sqrt{g} \{ (x + 4w)A_1 + (y - 8w)B_1 \\
&+ (\frac{5}{4}x - \frac{7}{16}y + 10z + 16w)P_4 + (\frac{3}{2}x - \frac{9}{8}y + 10z + 24w)P_5 + \text{other invariants} \} \quad , \quad (51)
\end{aligned}$$

where "other invariants" means other than A_1, B_1, P_4 and P_5 . Now we see how nicely we have chosen the four graphs in Sec.5.

(i)

We note that the trivial terms are written in the total derivative form, therefore they do not contain any one of A_1, B_1, P_4 and P_5 .

(ii)

Now we know, from App.D,

$$\begin{aligned}
P_4|_{(\partial\partial h)^3} &= -\frac{1}{4}(\text{Graph1}) + \text{other } (\partial\partial h)^3\text{-terms} \quad , \\
P_5|_{(\partial\partial h)^3} &= \frac{1}{4}(\text{Graph2}) + \text{other } (\partial\partial h)^3\text{-terms} \quad , \\
A_1|_{(\partial\partial h)^3} &= -(\text{Graph3}) + \text{other } (\partial\partial h)^3\text{-terms} \quad , \\
B_1|_{(\partial\partial h)^3} &= -\frac{1}{4}(\text{Graph3}) + \frac{1}{4}(\text{Graph67}) + \text{other } (\partial\partial h)^3\text{-terms} \quad , \quad (52)
\end{aligned}$$

where "other $(\partial\partial h)^3$ -terms" means "other terms than Graph1,2,3 and 67".[43]

(iii)

We also note, again from App.D, Graphs1,2,3 and 67 do not come from other invariants than (A_1, B_1, P_4, P_5) .

These properties are due to the chosen four graphs. Then we can rewrite (51) as

$$\begin{aligned}
G(x, x; t)|_{t^0, (\partial\partial h)^3} &= \frac{1}{(4\pi)^3} \{ (-x - \frac{1}{4}y - 2w)(\text{Graph3}) + \frac{1}{4}(y - 8w)(\text{Graph67}) \\
&+ \frac{1}{4}(\frac{3}{2}x - \frac{9}{8}y + 10z + 24w)(\text{Graph2}) - \frac{1}{4}(\frac{5}{4}x - \frac{7}{16}y + 10z + 16w)(\text{Graph1}) \\
&+ \text{other } (\partial\partial h)^3\text{-terms} \} \quad . \quad (53)
\end{aligned}$$

Comparing the result of Sec.5, we finally obtain

$$\begin{aligned}
x &= -\frac{83}{189 \times 60} \quad , \quad y = \frac{31}{189 \times 15} \quad , \quad z = -\frac{11}{189 \times 50} \quad , \quad w = \frac{3}{189 \times 10} \quad , \\
G(x, x; t)|_{t^0} &= -2g^{\mu\nu} < T_{\mu\nu} > = \frac{1}{(4\pi)^3} \frac{1}{189} \sqrt{g} \{ -\frac{83}{60}C_1 + \frac{31}{15}C_2 - \frac{11}{50}C_3 + \frac{3}{10}E + \text{trivial terms} \} \quad . \quad (54)
\end{aligned}$$

The trivial terms can be similarly obtained, but they do change by introducing the local counterterms in the action and seem to be unimportant. This result (54) is similar to that of Ref.[16].

7 Discussion and Conclusion

We have presented a new algorithm to obtain the Weyl anomaly in the higher-dimensions. The Feynman rules in coordinate space are presented. The graphical representation is exploited at all stages. Especially the graphical calculation is taken to efficiently compute the coefficients of the four graphs given in Sec.5. Explicit result of the Weyl anomaly for the 6 dim scalar-gravity is obtained.

As the space-time dimension increases, the number of suffixes to deal with increases because we must treat higher products of Riemann tensors. The aid of the computer is indispensable in this algebraic calculation. As mentioned at some places in the text and the appendices, the weight calculation in the contraction of multi-suffixed quantities relies on a computer (a C-program[37]). Although we do not touch on the computer algorithm in the present paper, it helps to obtain the concrete results.

In the recent rapid development of string theory, the low-energy effective actions play an important role. They are field theories (supergravities) on various (higher) dimensions. The chiral anomalies of gravitational and gauge symmetries were well analyzed for those low-energy effective actions. The famous one is the pioneering work by Green and Schwarz[44] where they found the $SO(32)$ and $E_8 \times E_8$ gauge group from the analysis of the chiral anomaly structure of 10 dim $N=1$ supergravity. Clearly the analysis from the Weyl anomaly side is lacking. From the present standpoint, we stress the importance of examining the string from the structure of the Weyl anomaly in the low-energy effective theories.[45] One reason is we know some important models often have vanishing Weyl anomaly due to conformal symmetry. Another is that the supersymmetry surely relates the Weyl anomaly to the chiral one. We can examine the role of supersymmetry from this point. We hope the present result will become useful when we go over the quantum field theory through the string theory.

We have most experience with quantization only in 0 to 4 dim field theories. Higher dimensional quantum field theories have not been so thoroughly examined (at least systematically) so far, because they are unrenormalizable except for free theories. In the text we consider free theories on curved space. It is meaningful if we ignore the trivial terms and the the divergent massive terms, which should be explained by the quantum gravitational mode. It might be possible to find a clue to make meaningful the higher dimensional field theories through the present analysis.

Although the non-perturbative aspect is recently stressed in string theory, the perturbative analysis is still important because it is one of few reliable approaches to analyze dynamical aspects systematically. We suppose the analysis will become important to understand how

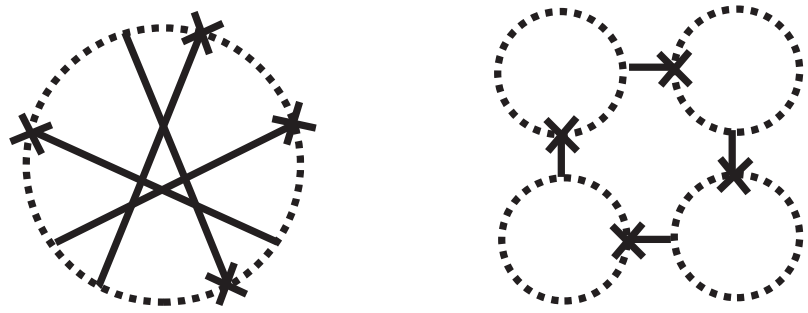


Fig.10 Two important $(\partial\partial h)^4$ -graphs in 8 dim.

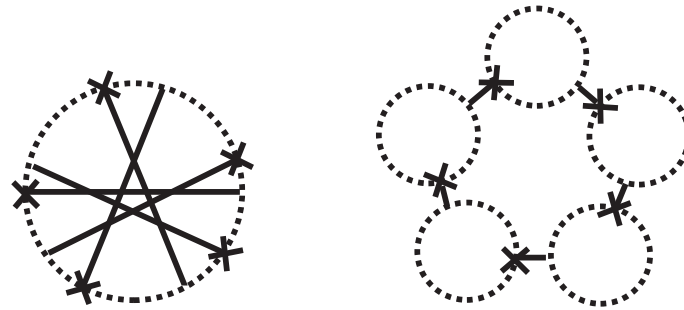


Fig.11 Two important $(\partial\partial h)^5$ -graphs in 10 dim.

the quantum field theory is generalized in the coming new era of Planck physics. Finally we point out that the graphs shown in Fig.10 and Fig.11 are expected to become some of the "important graphs" in the Weyl anomaly calculation in 8 dim and 10 dim respectively.

Acknowledgment

The authors thank Prof. M. Creutz for reading the manuscript carefully. One of the authors (S.I.) thanks the hospitality at Physics Department, Brookhaven National Laboratory where this work is finished.

Appendix A. Propagator Rules

$G_0(x; t)$ is the solution of the heat equation Eq.(13) and is given by

$$G_0(x; t) = \frac{1}{(4\pi t)^{n/2}} e^{-\frac{x^2}{4t}} I_N \quad , \quad t > 0 \quad , \quad x^2 = (x_1)^2 + (x_2)^2 + \cdots + (x_n)^2 \quad , \quad (55)$$

where I_N is the $N \times N$ unit matrix and $x = (x_1, x_2, \dots, x_n)$ is the n-dim Euclidean space coordinates. It has the basic properties:

$$\begin{aligned} G_0(x; t) &= G_0(-x; t) : \text{even function of } x \quad , \\ G_0(\sqrt{a}x; at) &= a^{-\frac{n}{2}} G_0(x; t) \quad , \quad a > 0 \quad . \end{aligned} \quad (56)$$

The integral formula is given by

$$\int d^n x \ x^{\mu_1} \cdots x^{\mu_{2s}} G_0(x; t) = [\mu_1 \cdots \mu_{2s}] (2t)^s I_N \quad , \quad (57)$$

where $[\mu_1 \cdots \mu_{2s}]$ is the totally symmetric sum of products of Kronecker's deltas and is concretely defined by

$$\begin{aligned} [\mu\nu] &\equiv \delta^{\mu\nu} \quad , \\ [\mu\nu\lambda\sigma] &\equiv \delta^{\mu\nu}\delta^{\lambda\sigma} + \delta^{\mu\sigma}\delta^{\nu\lambda} + \delta^{\mu\lambda}\delta^{\nu\sigma} \quad , \\ [\mu_1 \cdots \mu_6] &\equiv \delta^{\mu_1\mu_2}[\mu_3 \cdots \mu_6] + \delta^{\mu_1\mu_3}[\cdots] + \cdots + \delta^{\mu_1\mu_6}[\cdots] \quad , \\ &\cdots \\ &\cdots \\ [\mu_1 \cdots \mu_{2s}] &\equiv \delta^{\mu_1\mu_2}[\mu_3 \cdots \mu_{2s}] + \delta^{\mu_1\mu_3}[\cdots] + \cdots + \delta^{\mu_1\mu_{2s}}[\cdots] \quad . \end{aligned} \quad (58)$$

$G_0(x, t)$ has the "convolution" property.

Propagator Rule 1

$$G_0(v - w; r - k)G_0(w - u; k - l) = G_0(\bar{w}; \frac{(r-k)(k-l)}{r-l})G_0(v - u; r - l) \quad ,$$

$$r > k > l \quad , \quad \bar{w} = w - \frac{(k-l)v + (r-k)u}{r-l} \quad . \quad (59)$$

This relation is geometrically expressed in the coordinate space as in Fig.12. Some special cases of above are given by

Propagator Rule 2 , $v = 0, r = 1$ in Eq.(59)

$$G_0(w; 1 - k)G_0(w - u; k - l) = G_0(\bar{w}; \frac{(1-k)(k-l)}{1-l})G_0(u; 1 - l) \quad ,$$

$$1 > k > l \quad , \quad \bar{w} = w - \frac{1-k}{1-l}u \quad . \quad (60)$$

Propagator Rule 3 , $u = 0, l = 0$ in Eq.(59)

$$G_0(v - w; r - k)G_0(w; k) = G_0(\bar{w}; \frac{(r-k)k}{r})G_0(v; r) \quad ,$$

$$r > k > 0 \quad , \quad \bar{w} = w - \frac{k}{r}v \quad . \quad (61)$$

Propagator Rule 4 , $u = 0, v = 0, l = 0$, in Eq.(59)

$$G_0(w; r - k)G_0(w; k) = \frac{1}{(4\pi r)^{n/2}} G_0(w; \frac{(r-k)k}{r}) \quad , \quad r > k > 0 \quad . \quad (62)$$

The above three relations are geometrically represented as in Fig.13-15.

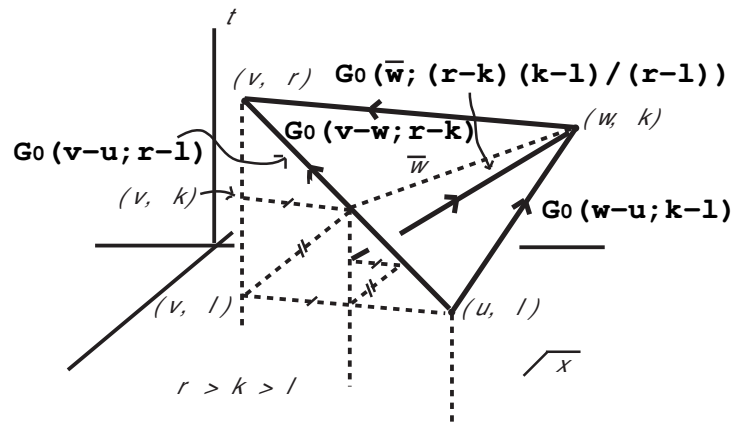


Fig.12 Propagator Rule 1, Eq.(59).

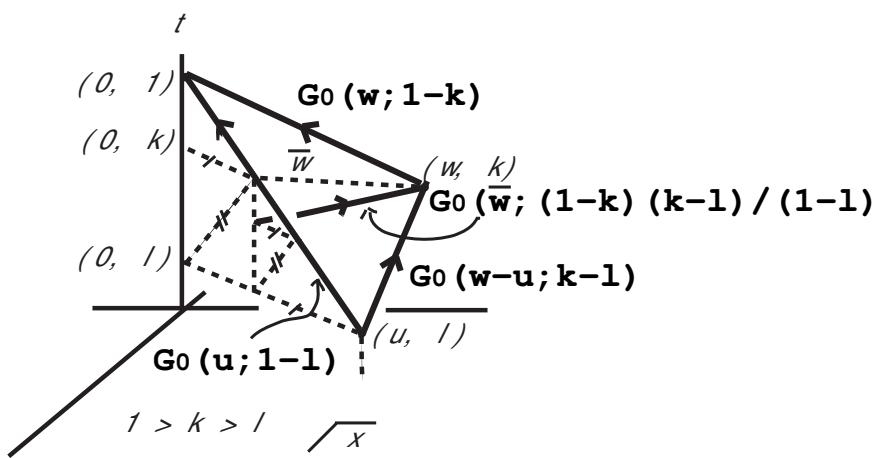


Fig.13 Propagator Rule 2, Eq.(60).

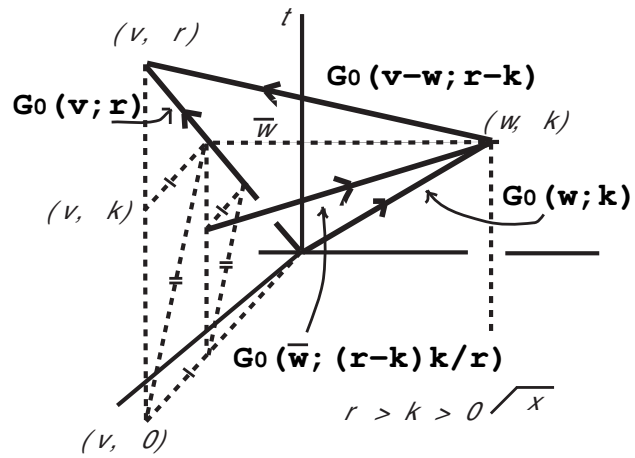


Fig.14 Propagator Rule 3, Eq.(61).

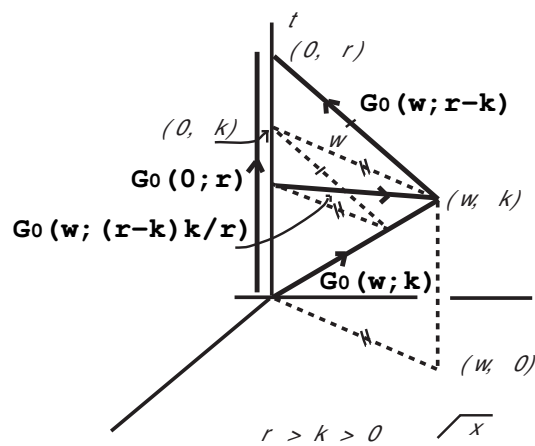


Fig.15 Propagator Rule 4, Eq.(62).

Appendix B. Supplementary Calculation of Sec.5

In Sec.5 of the text, we have evaluated $G(x, x; t)|_{t^0}$ focusing on 4 special $(\partial\partial h)^3$ -terms(graphs) in order to fix 4 coefficients of the main Weyl anomaly terms given in (49). Among the four graphs, Graph3 and 67 only are explained for simplicity. We evaluate the remaining graphs, Graph1 and 2 to supplement Sec.5.

From (36),

$$\begin{aligned}
G_3(x, x; t)|_{t^0} &= \frac{1}{(4\pi)^3} \int d^6\bar{w} \int d^6\bar{w} \int d^6w \int_0^1 dr'' \int_0^{r''} dr' \int_0^{r'} dr \\
&\times G_0(\bar{w}; \frac{(1-r'')(r''-r')}{1-r'}) G_0(\bar{w}; \frac{(1-r')(r'-r)}{1-r}) G_0(w; (1-r)r) \\
&\times V_0(x, w''; w''-w', r''-r') V_0(x, w'; w'-w, r'-r) V_0(x, w; w, r) + \text{irrel.} \\
&w'' = \bar{w} + R_2\bar{w} + R_3w \quad , \quad w''-w' = \bar{w} - S_2\bar{w} - T_1w \quad , \\
&w' = \bar{w} + R_1w \quad , \quad w'-w = \bar{w} - S_1w \quad , \quad (63)
\end{aligned}$$

where R_i, S_i and T_1 are defined in (37). Because Graph1 and 2 do not have tadpoles and  subgraph, we can reduce V_0 of (71) with (72) to the following relevant form.

$$V_0(x, v; w, r) = -\frac{1}{2} \times \frac{1}{4r^2} \times \begin{array}{c} \text{Diagram: two vertices } v \text{ and } w \text{ connected by a solid line, with a dashed line } w \text{ entering from the left and a dashed line } v \text{ exiting to the right.} \end{array} + \frac{1}{2r} \begin{array}{c} \text{Diagram: a vertical solid line with a dashed loop attached to its right end. The loop has vertices } v \text{ and } w. \end{array} + \text{irrel. terms} \quad . \quad (64)$$

The first V_0 in (63) is evaluated as

$$\begin{aligned}
V_0(x, w''; w''-w', r''-r') &= -\frac{1}{8(r''-r')^2} \times \begin{array}{c} \text{Diagram: two vertices } \bar{w}+R_2\bar{w}+R_3w \text{ and } \bar{w}+R_2\bar{w}+R_3w \text{ connected by a solid line, with a dashed line } \bar{w}-S_2\bar{w}-T_1w \text{ entering from the left and a dashed line } \bar{w}-S_2\bar{w}-T_1w \text{ exiting to the right.} \end{array} \\
&+ \frac{1}{2(r''-r')} \times \begin{array}{c} \text{Diagram: a vertical solid line with a dashed loop attached to its right end. The loop has vertices } \bar{w}+R_2\bar{w}+R_3w \text{ and } \bar{w}-S_2\bar{w}-T_1w. \end{array} + \text{irrel. terms} \quad , \quad (65)
\end{aligned}$$

$$\text{second term of (65)} = \frac{1 \times (-1)}{2(r''-r')} \times \begin{array}{c} \text{Diagram: a vertical solid line with a dashed loop attached to its right end. The loop has vertices } R_2\bar{w}+R_3w \text{ and } S_2\bar{w}+T_1w. \end{array} + \text{irrel. terms} \quad ,$$

$$\begin{aligned}
\text{first term of (65)} &= -\frac{1}{8(r''-r')^2} \left(2 \times 2 \times (-1) \times \begin{array}{c} \text{Diagram: two vertices } \bar{w} \text{ and } R_2\bar{w}+R_3w \text{ connected by a solid line, with a dashed line } S_2\bar{w}+T_1w \text{ entering from the left and a dashed line } R_2\bar{w}+R_3w \text{ exiting to the right.} \end{array} + \begin{array}{c} \text{Diagram: two vertices } R_2\bar{w}+R_3w \text{ and } R_2\bar{w}+R_3w \text{ connected by a solid line, with a dashed line } S_2\bar{w}+T_1w \text{ entering from the left and a dashed line } R_2\bar{w}+R_3w \text{ exiting to the right.} \end{array} \right) \\
&+ \text{irrel. terms} \quad . \quad (66)
\end{aligned}$$

The above V_0 , with the \bar{w} -integration, gives

$$\begin{aligned}
\int d^6\bar{w} V_0(x, w''; w'' - w', r'' - r') &= -\frac{1}{8(r'' - r')^2} \times \\
&+ \left\{ \frac{-1}{2(r'' - r')} + \frac{2 \times 2}{8(r'' - r')^2} \times 2 \frac{(1 - r'')(r'' - r')}{(1 - r')} \right\} \\
&\quad \begin{array}{c} \text{Graph 1} \\ \text{Graph 2} \end{array} + \text{irrel. terms} \\
&= -\frac{(R_2)^2(S_2)^2}{8(r'' - r')^2} \times \begin{array}{c} \text{Graph 3} \end{array} + \frac{1 + r' - 2r''}{2(r'' - r')(1 - r')} R_2 S_2 \times \\
&\quad \begin{array}{c} \text{Graph 4} \end{array} + \text{irrel. terms} , \quad (67)
\end{aligned}$$

where \bar{w} is integrated out and the relations $R_3/R_2 = T_1/S_2 = R_1$ are used. Therefore the $V_0 V_0 V_0$ -part of (63), with the \bar{w} -integration, can be written as

$$\begin{aligned}
\int d^6\bar{w} V_0(x, w''; w'' - w', r'' - r') V_0(x, w'; w' - w, r' - r) V_0(x, w; w, r) &= \\
&\left\{ -\frac{(1 - r'')^2}{8(1 - r')^4} \times \begin{array}{c} \text{Graph 5} \end{array} + \frac{(1 + r' - 2r'')(1 - r'')}{2(1 - r')^3} \times \begin{array}{c} \text{Graph 6} \end{array} \right\} \\
&\times \left\{ -\frac{1}{8(r' - r)^2} \times \begin{array}{c} \text{Graph 7} \end{array} + \frac{1}{2(r' - r)} \times \begin{array}{c} \text{Graph 8} \end{array} \right\} \\
&\times \left\{ -\frac{1}{8r^2} \times \begin{array}{c} \text{Graph 9} \end{array} + \frac{1}{2r} \times \begin{array}{c} \text{Graph 10} \end{array} \right\} \\
&+ \text{irrel.} . \quad (68)
\end{aligned}$$

Now we can further evaluate (63) by picking up relevant powers of \bar{w} in (68) in the same way as Sec.5. After integration of the remaining coordinates (\bar{w}, w) and the parameters (r, r', r'') , the final result is

$$G_3(x, x; t)|_{t^0} = \frac{1}{(4\pi)^3} \left\{ \frac{1}{36 \times 630} (\text{Graph1}) + \frac{1}{36 \times 35} (\text{Graph2}) \right\} + \text{other terms} . \quad (69)$$

$$\begin{aligned}
W^{\mu\nu} &= - \underset{\mu}{\text{---}} \underset{\nu}{\text{---}} \times \dots + \underset{\mu}{\text{---}} \underset{\nu}{\text{---}} \times \underset{\nu}{\text{---}} \underset{\mu}{\text{---}} - \underset{\mu}{\text{---}} \underset{\nu}{\text{---}} \times \underset{\nu}{\text{---}} \underset{\mu}{\text{---}} + O(h^4) \\
N_\lambda &= - \underset{\lambda}{\text{---}} \underset{\lambda}{\text{---}} \text{---} \text{---} \text{---} + \underset{\lambda}{\text{---}} \underset{\lambda}{\text{---}} \text{---} \text{---} \text{---} + \underset{\lambda}{\text{---}} \underset{\lambda}{\text{---}} \text{---} \text{---} \text{---} \\
&- \underset{\lambda}{\text{---}} \underset{\lambda}{\text{---}} \text{---} \text{---} \text{---} - \underset{\lambda}{\text{---}} \underset{\lambda}{\text{---}} \text{---} \text{---} \text{---} - \underset{\lambda}{\text{---}} \underset{\lambda}{\text{---}} \text{---} \text{---} \text{---} \\
&+ O(h^4)
\end{aligned}$$

Fig.16 $W^{\mu\nu}$ and N_λ .

Appendix C. Weak Field Expansion of 6 Dim Scalar-Gravity Theory

In the text, we have taken 6 dim scalar-gravity theory (1) as an higher-dimensional model. The expressions for the general theories are expressed in terms of $W_{\mu\nu}$, N_λ and M (10). In this appendix we graphically express those general expressions for the case of the explicit model.

C.1 Graphs of W, N and M

For the 6 dim scalar-gravity theory, $W_{\mu\nu}$, N_λ and M are given by (11). Their weak-field expansions ($g_{\mu\nu} = \delta_{\mu\nu} + h_{\mu\nu}$) up to $O(h^3)$ are given in Fig.16 for $W_{\mu\nu}$ and N_λ , and in Fig.17-21 for M . Especially they are classified by the number of closed suffix-loops.

$$M = Mh + Mhh + Mhh + O(h^4)$$

$$Mh = -\frac{1}{20} \begin{array}{c} \text{Diagram: two circles connected by a vertical line with a cross at the center, and a horizontal line connecting the two circles.} \end{array} - \frac{1}{5} \begin{array}{c} \text{Diagram: two circles connected by a vertical line with a cross at the center, and a horizontal line connecting the two circles.} \end{array}$$

Fig.17 M , Order of h .

$$Mhh = Mhh2 + Mhh1 + Mhh0$$

$$Mhh2 = \frac{1}{20} \begin{array}{c} \text{Diagram: two circles connected by a vertical line with a cross at the center, and a horizontal line connecting the two circles.} \end{array} + \frac{1}{20} \begin{array}{c} \text{Diagram: two circles connected by a vertical line with a cross at the center, and a horizontal line connecting the two circles.} \end{array} - \frac{1}{80} \begin{array}{c} \text{Diagram: two circles connected by a vertical line with a cross at the center, and a horizontal line connecting the two circles.} \end{array}$$

$$Mhh1 = \frac{1}{10} \begin{array}{c} \text{Diagram: two circles connected by a vertical line with a cross at the center, and a horizontal line connecting the two circles.} \end{array} - \frac{2}{5} \begin{array}{c} \text{Diagram: two circles connected by a vertical line with a cross at the center, and a horizontal line connecting the two circles.} \end{array} + \frac{1}{20} \begin{array}{c} \text{Diagram: two circles connected by a vertical line with a cross at the center, and a horizontal line connecting the two circles.} \end{array}$$

$$Mhh0 = \frac{1}{10} \begin{array}{c} \text{Diagram: two circles connected by a vertical line with a cross at the center, and a horizontal line connecting the two circles.} \end{array} + \frac{1}{5} \begin{array}{c} \text{Diagram: two circles connected by a vertical line with a cross at the center, and a horizontal line connecting the two circles.} \end{array}$$

Fig.18 M , Order of h^2 .

$$M_{hhh} = M_{hhh2} + M_{hhh1} + M_{hhh0}$$

$$M_{hhh2} = \frac{3}{20} \begin{array}{c} \text{Diagram 1: Two loops with crosses, one solid, one dashed, connected by a vertical line with a cross. The solid loop has an arrow pointing down. The dashed loop has an arrow pointing up.} \end{array} + \frac{3}{20} \begin{array}{c} \text{Diagram 2: Two loops with crosses, one solid, one dashed, connected by a vertical line with a cross. The solid loop has an arrow pointing up. The dashed loop has an arrow pointing down.} \end{array} - \frac{1}{20} \begin{array}{c} \text{Diagram 3: Two loops with crosses, one solid, one dashed, connected by a vertical line with a cross. The solid loop has an arrow pointing down. The dashed loop has an arrow pointing down.} \end{array}$$

$$+ \frac{3}{40} \begin{array}{c} \text{Diagram 4: Two loops with crosses, one solid, one dashed, connected by a vertical line with a cross. The solid loop has an arrow pointing down. The dashed loop has an arrow pointing up. A dashed box encloses the two loops.} \end{array} + \frac{1}{16} \begin{array}{c} \text{Diagram 5: Two loops with crosses, one solid, one dashed, connected by a vertical line with a cross. The solid loop has an arrow pointing up. The dashed loop has an arrow pointing up. A dashed box encloses the two loops.} \end{array}$$

Fig.19 M , Order of h^3 and loop no=2.

$$\begin{aligned}
M_{hhh1} = & -\frac{4}{5} \text{ (Diagram 1)} - \frac{1}{5} \text{ (Diagram 2)} - \frac{1}{5} \text{ (Diagram 3)} \\
& - \frac{1}{10} \text{ (Diagram 4)} - \frac{3}{20} \text{ (Diagram 5)} - \frac{1}{20} \text{ (Diagram 6)} \\
& - \frac{1}{20} \text{ (Diagram 7)}
\end{aligned}$$

Diagrams are represented by dotted lines with crosses and arrows. Diagram 1: two vertical lines with crosses, one on top of the other, with a dotted circle around them. Diagram 2: a horizontal line with a cross, with a dotted circle around it. Diagram 3: a vertical line with a cross, with a dotted circle around it. Diagram 4: a vertical line with a cross, with a dotted circle around it. Diagram 5: a vertical line with a cross, with a dotted circle around it. Diagram 6: a horizontal line with a cross, with a dotted circle around it. Diagram 7: a vertical line with a cross, with a dotted circle around it.

Fig.20 M , Order of h^3 and loop no=1.

$$\begin{aligned}
M_{hh0} = & -\frac{1}{5} \text{ (Diagram 1)} - \frac{1}{5} \text{ (Diagram 2)} \\
& - \frac{1}{10} \text{ (Diagram 3)} - \frac{2}{5} \text{ (Diagram 4)}
\end{aligned}$$

Diagrams are represented by dotted lines with crosses and arrows. Diagram 1: two vertical lines with crosses, one on top of the other, with a dotted circle around them. Diagram 2: a horizontal line with a cross, with a dotted circle around it. Diagram 3: a vertical line with a cross, with a dotted circle around it. Diagram 4: a horizontal line with a cross, with a dotted circle around it.

Fig.21 M , Order of h^3 and loop no=0.

C.2 Taylor Expansion of W,N and M

In Sec.4 of the text, we have Taylor-expanded $W_{\mu\nu}$, N_μ and M , which are the background-functional appearing in the differential operator \vec{D} .

$$\begin{aligned} W_{\mu\nu}(x+v) &= W_{\mu\nu}(x) + \partial_{\alpha_1} W_{\mu\nu} \cdot v^{\alpha_1} + \frac{1}{2} \partial_{\alpha_1} \partial_{\alpha_2} W_{\mu\nu} \cdot v^{\alpha_1} v^{\alpha_2} + \dots , \\ N_\mu(x+v) &= N_\mu(x) + \partial_{\alpha_1} N_\mu \cdot v^{\alpha_1} + \frac{1}{2} \partial_{\alpha_1} \partial_{\alpha_2} N_\mu \cdot v^{\alpha_1} v^{\alpha_2} + \dots , \\ M(x+v) &= M(x) + \partial_{\alpha_1} M \cdot v^{\alpha_1} + \frac{1}{2} \partial_{\alpha_1} \partial_{\alpha_2} M \cdot v^{\alpha_1} v^{\alpha_2} + \dots . \end{aligned} \quad (70)$$

We focus on those terms which have only $\partial\partial h$ -type ones. They are sufficient to determine the Weyl anomaly, and are used in the text.

(i) Expansion Terms appearing in V_0 of (33)

$$V_0(x, v; w, r) = \frac{1}{2!} \partial_{\alpha_1} \partial_{\alpha_2} W_{\mu\nu} \cdot v^{\alpha_1} v^{\alpha_2} \left(-\frac{\delta_{\mu\nu}}{2r} + \frac{w_\mu w_\nu}{4r^2} \right) + \partial_{\alpha_1} N_\mu \cdot v^{\alpha_1} \left(-\frac{w_\mu}{2r} \right) + M \quad . \quad (71)$$

$$\begin{aligned} \frac{1}{2!} \partial_{\alpha_1} \partial_{\alpha_2} W_{\mu\nu} \cdot v^{\alpha_1} v^{\alpha_2} &= -\frac{1}{2} \text{Diagram: two vertical lines with a dot between them, each with a dot at the top and a dot at the bottom, labeled } \mu \text{ and } \nu \text{ at the bottom.} + \text{irrel. terms} , \\ \partial_{\alpha_1} N_\lambda \cdot v^{\alpha_1} &= -\text{Diagram: a vertical line with a dot at the top and a dot at the bottom, labeled } \lambda \text{ at the bottom.} + \text{irrel. terms} , \\ M &= -\frac{1}{20} \text{Diagram: a circle with a dot at the top and a dot at the bottom, labeled } \lambda \text{ at the bottom.} - \frac{1}{5} \text{Diagram: a circle with a dot at the top and a dot at the bottom, labeled } \nu \text{ at the top.} + \text{irrel. terms} . \end{aligned} \quad (72)$$

(ii) Expansion Terms appearing in V_1 of (33)

$$\begin{aligned} V_1(x, v; w, r) &= \frac{1}{4!} \partial_{\alpha_1} \partial_{\alpha_2} \dots \partial_{\alpha_4} W_{\mu\nu} \cdot v^{\alpha_1} v^{\alpha_2} \dots v^{\alpha_4} \left(-\frac{\delta_{\mu\nu}}{2r} + \frac{w_\mu w_\nu}{4r^2} \right) \\ &\quad + \frac{1}{3!} \partial_{\alpha_1} \partial_{\alpha_2} \partial_{\alpha_3} N_\mu \cdot v^{\alpha_1} v^{\alpha_2} v^{\alpha_3} \left(-\frac{w_\mu}{2r} \right) + \frac{1}{2!} \partial_{\alpha_1} \partial_{\alpha_2} M \cdot v^{\alpha_1} v^{\alpha_2} \quad . \end{aligned} \quad (73)$$

$$\frac{1}{4!} \partial_{\alpha_1} \partial_{\alpha_2} \cdots \partial_{\alpha_4} W_{\mu\nu} \cdot v^{\alpha_1} v^{\alpha_2} \cdots v^{\alpha_4} = -\frac{1}{2} \left[\begin{array}{c} \text{Diagram: Four vertical lines } \nu \text{ meeting at a cross} \\ \text{at } \mu \text{ and } v \end{array} \right] + \text{irrel. terms} ,$$

$$\frac{1}{3!} \partial_{\alpha_1} \partial_{\alpha_2} \partial_{\alpha_3} N_{\lambda} \cdot v^{\alpha_1} v^{\alpha_2} v^{\alpha_3} = -\frac{1}{2} \left[\begin{array}{c} \text{Diagram: Three vertical lines } \nu \text{ meeting at a cross} \\ \text{at } \lambda \text{ and a loop} \\ \text{Diagram: Three vertical lines } \nu \text{ meeting at a cross} \\ \text{at } \lambda \text{ and a loop} \end{array} \right]$$

$$\begin{aligned} & + \text{irrel. terms} , \\ & \frac{1}{2!} \partial_{\alpha_1} \partial_{\alpha_2} M \cdot v^{\alpha_1} v^{\alpha_2} = \\ & \frac{1}{2} \left[\begin{array}{c} \text{Diagram: Two vertical lines } \nu \text{ meeting at a cross} \\ \text{at } \frac{1}{20} \text{ and a loop} \\ \text{Diagram: Two vertical lines } \nu \text{ meeting at a cross} \\ \text{at } \frac{1}{20} \text{ and a loop} \\ \text{Diagram: Two vertical lines } \nu \text{ meeting at a cross} \\ \text{at } -\frac{2}{80} \text{ and a loop} \\ \text{Diagram: Two vertical lines } \nu \text{ meeting at a cross} \\ \text{at } \frac{2}{10} \text{ and a loop} \\ \text{Diagram: Two vertical lines } \nu \text{ meeting at a cross} \\ \text{at } -\frac{2}{5} \text{ and a loop} \\ \text{Diagram: Two vertical lines } \nu \text{ meeting at a cross} \\ \text{at } \frac{2}{20} \text{ and a loop} \\ \text{Diagram: Two vertical lines } \nu \text{ meeting at a cross} \\ \text{at } \frac{2}{10} \text{ and a loop} \\ \text{Diagram: Two vertical lines } \nu \text{ meeting at a cross} \\ \text{at } \frac{2}{5} \text{ and a loop} \end{array} \right] \\ & + \text{irrel. terms} . \end{aligned} \quad (74)$$

(iii) Expansion Terms appearing in V_2 of (33)

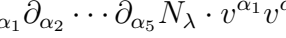
$$\begin{aligned} V_2(x, v; w, r) = & \frac{1}{6!} \partial_{\alpha_1} \partial_{\alpha_2} \cdots \partial_{\alpha_6} W_{\mu\nu} \cdot v^{\alpha_1} v^{\alpha_2} \cdots v^{\alpha_6} \left(-\frac{\delta_{\mu\nu}}{2r} + \frac{w_{\mu} w_{\nu}}{4r^2} \right) \\ & + \frac{1}{5!} \partial_{\alpha_1} \partial_{\alpha_2} \cdots \partial_{\alpha_5} N_{\mu} \cdot v^{\alpha_1} v^{\alpha_2} \cdots v^{\alpha_5} \left(-\frac{w_{\mu}}{2r} \right) \\ & + \frac{1}{4!} \partial_{\alpha_1} \partial_{\alpha_2} \cdots \partial_{\alpha_4} M \cdot v^{\alpha_1} v^{\alpha_2} \cdots v^{\alpha_4} . \end{aligned} \quad (75)$$

$$\frac{1}{6!} \partial_{\alpha_1} \partial_{\alpha_2} \cdots \partial_{\alpha_6} W_{\mu\nu} \cdot v^{\alpha_1} v^{\alpha_2} \cdots v^{\alpha_6} = -\frac{3}{4} \text{ (Diagram)} + \text{irrel. terms} \quad ,$$

$$\frac{1}{5!} \partial_{\alpha_1} \partial_{\alpha_2} \cdots \partial_{\alpha_5} N_\lambda \cdot v^{\alpha_1} v^{\alpha_2} \cdots v^{\alpha_5} =$$

$\frac{1}{2} \left[$

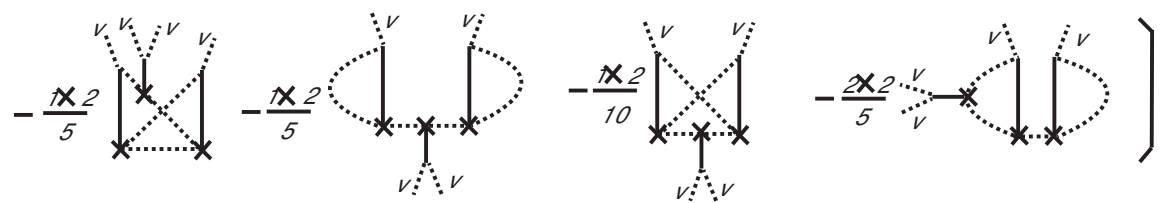

$-$


$-$


$\right]$

$$\begin{aligned}
 & + \text{irrel. terms} , \\
 & \frac{1}{4!} \partial_{\alpha_1} \partial_{\alpha_2} \cdots \partial_{\alpha_4} M \cdot v^{\alpha_1} v^{\alpha_2} \cdots v^{\alpha_4} = \\
 & \frac{1}{2} \left(\frac{3}{20} \text{Diagram A} + \frac{3}{20} \text{Diagram B} - \frac{1}{20} \text{Diagram C} + \frac{3x_2}{40} \text{Diagram D} + \frac{3x_2}{16} \text{Diagram E} \right)
 \end{aligned}$$

$$-\frac{3x^2}{20} - \frac{7x^2}{20} - \frac{1x^2}{20}$$



+irrel. terms . (76)

Appendix D. Weak-Expansion of Invariants with (Mass)⁶-Dim

In 6 dim space, there are totally 17 independent general invariants given in (50). In this appendix, we list the coefficients of $(\partial\partial h)^3$ -terms when the invariants are weak-field-expanded ($g_{\mu\nu} = \delta_{\mu\nu} + h_{\mu\nu}$). They are obtained by a computer using a C-program[37]. Among 17 ones, $O_i (i = 1 \sim 4)$ terms do not have $(\partial\partial h)^3$ -terms. As shown in the first column of the table, there are 90 independent $(\partial\partial h)^3$ -terms. Some terms (G3,G67,G1,G2) are given, in the ordinary literal form, in (39) and graphically in Fig.9. Their complete list is graphically given in [46]. For example the A_1 column says

$$\begin{aligned}
A_1(R_{\mu\nu\lambda\sigma} R^{\sigma\lambda}_{\tau\omega} R^{\omega\tau\nu\mu}) = & (-1) \times \text{Graph3}(\partial_\sigma \partial_\tau h_{\mu\nu} \cdot \partial_\nu \partial_\lambda h_{\tau\omega} \cdot \partial_\omega \partial_\mu h_{\lambda\sigma}) \\
& + (-3) \times \text{Graph13}(\partial_\mu \partial_\nu h_{\tau\sigma} \cdot \partial_\mu \partial_\omega h_{\lambda\sigma} \cdot \partial_\tau \partial_\omega h_{\nu\lambda}) \\
& + (1) \times \text{Graph14}(\partial_\mu \partial_\nu h_{\omega\sigma} \cdot \partial_\nu \partial_\lambda h_{\tau\omega} \cdot \partial_\lambda \partial_\mu h_{\sigma\tau}) \\
& + (3) \times \text{Graph15}(\partial_\mu \partial_\nu h_{\omega\sigma} \cdot \partial_\tau \partial_\omega h_{\nu\lambda} \cdot \partial_\lambda \partial_\mu h_{\sigma\tau}) + O(h^4) \quad .
\end{aligned} \tag{77}$$

The content of the table is fully used in Sec.5 and 6 of the text. Especially the choice of the four graphs of Fig.9 relies on the table.

Graph	P_1	P_2	P_3	P_4	P_5	P_6	A_1	B_1	T_1	T_2	T_3	T_4	S
$G1$	0	0	0	$-\frac{1}{4}$	0	0	0	0	0	0	0	0	0
$G2$	0	0	0	0	$\frac{1}{4}$	0	0	0	0	0	0	0	0
$G3$	0	0	0	0	0	0	-1	$-\frac{1}{4}$	0	0	0	0	0
$G4$	0	0	0	$-\frac{3}{4}$	0	0	0	0	0	0	0	-2	-4
$G5$	0	0	0	0	0	$\frac{1}{2}$	0	0	0	0	0	-1	-2
$G6$	0	0	0	0	0	$\frac{1}{2}$	0	0	0	-1	0	0	0
$G7$	0	0	0	0	0	0	0	$\frac{3}{2}$	0	0	2	0	0
$G8$	0	0	0	0	$\frac{1}{2}$	0	0	0	0	-1	0	0	0
$G9$	0	0	0	0	0	$\frac{1}{2}$	0	0	0	0	0	0	0
$G10$	0	0	0	0	$\frac{1}{4}$	0	0	0	0	-1	0	0	-8
$G11$	0	0	0	0	0	$\frac{1}{2}$	0	0	0	0	0	0	-16
$G12$	0	0	0	0	0	0	0	$\frac{3}{2}$	0	0	6	0	-8
$G13$	0	0	0	0	0	0	-3	$-\frac{3}{4}$	0	0	-2	0	-4

Table 1 Weak-Expansion of Invariants with (Mass)⁶-Dim.: $(\partial\partial h)^3$ -Part

G1-G13([No of suffix-loops]=1)

Graph	P_1	P_2	P_3	P_4	P_5	P_6	A_1	B_1	T_1	T_2	T_3	T_4	S
G_{14}	0	0	0	0	0	0	1	0	0	0	-1	0	12
G_{15}	0	0	0	0	0	0	3	0	0	0	-1	0	0
G_{16}	0	0	0	0	-1	0	0	0	0	1	0	-2	-4
G_{17}	0	0	0	0	0	$-\frac{1}{2}$	0	0	0	1	0	0	-16
G_{18}	0	0	0	0	0	0	0	$-\frac{3}{4}$	0	0	-1	0	-4
G_{19}	0	0	0	0	0	$-\frac{1}{2}$	0	0	0	$\frac{1}{2}$	0	$\frac{3}{2}$	7
G_{20}	0	0	0	0	0	0	0	$-\frac{3}{4}$	0	0	-2	0	6
G_{21}	0	0	0	0	0	$-\frac{1}{2}$	0	0	0	0	0	0	0
G_{22}	0	0	0	0	0	0	0	$-\frac{3}{2}$	0	0	-2	0	0
G_{23}	0	$-\frac{1}{2}$	0	0	0	0	0	0	-2	0	0	0	0
G_{24}	0	0	2	0	0	0	0	0	-1	0	0	0	0
G_{25}	0	0	0	0	0	$-\frac{1}{2}$	0	0	0	0	0	0	0
G_{26}	0	$-\frac{1}{2}$	0	0	0	0	0	0	0	0	0	0	0
G_{27}	0	0	0	$\frac{3}{8}$	0	0	0	0	0	0	0	1	2
G_{28}	0	0	0	0	0	$-\frac{1}{4}$	0	0	0	0	0	$\frac{1}{2}$	1
G_{29}	0	0	0	0	$-\frac{1}{2}$	0	0	0	0	$\frac{5}{4}$	0	0	8
G_{30}	0	0	0	0	0	$-\frac{1}{2}$	0	0	0	0	0	0	8
G_{31}	0	0	0	0	$-\frac{1}{2}$	0	0	0	0	$\frac{1}{4}$	0	0	0
G_{32}	0	0	0	$\frac{3}{4}$	0	0	0	0	0	0	0	1	2
G_{33}	0	0	0	$\frac{3}{8}$	0	0	0	0	0	0	0	1	2
G_{34}	0	0	0	0	0	$-\frac{1}{4}$	0	0	0	$\frac{1}{2}$	0	0	0
G_{35}	0	0	0	$\frac{3}{8}$	0	0	0	0	0	$-\frac{1}{4}$	0	0	-4
G_{36}	0	0	0	0	0	$-\frac{1}{4}$	0	0	0	$\frac{1}{2}$	$\frac{1}{2}$	0	-2
G_{37}	0	0	0	0	$-\frac{1}{2}$	0	0	0	0	$\frac{1}{2}$	0	0	-8
G_{38}	0	0	0	0	0	$-\frac{1}{2}$	0	0	0	0	1	0	-4
G_{39}	0	0	0	$\frac{3}{8}$	0	0	0	0	0	$-\frac{1}{4}$	0	1	-2
G_{40}	0	0	0	0	0	$-\frac{1}{4}$	0	0	0	0	$\frac{1}{2}$	$\frac{1}{2}$	-1
G_{41}	0	0	0	0	$-\frac{1}{2}$	0	0	0	0	$-\frac{1}{2}$	0	0	0
G_{42}	0	0	0	$\frac{3}{4}$	0	0	0	0	0	$-\frac{1}{2}$	0	0	0

Table 1 Weak-Expansion of Invariants with (Mass)⁶-Dim.: $(\partial\partial h)^3$ -Part

Graph	P_1	P_2	P_3	P_4	P_5	P_6	A_1	B_1	T_1	T_2	T_3	T_4	S
$G43$	0	0	0	0	$\frac{1}{4}$	0	0	0	0	$\frac{1}{2}$	0	0	-2
$G44$	0	0	0	$-\frac{3}{4}$	0	0	0	0	0	1	0	0	-8
$G45$	0	0	0	0	0	$\frac{1}{4}$	0	0	0	$-\frac{1}{2}$	$-\frac{1}{2}$	0	14
$G46$	0	0	0	0	0	$\frac{1}{4}$	0	0	0	$-\frac{1}{4}$	0	$-\frac{3}{4}$	$-\frac{7}{2}$
$G47$	0	0	0	0	0	$\frac{1}{4}$	0	0	0	$-\frac{1}{2}$	0	0	8
$G48$	0	0	0	0	$\frac{1}{2}$	0	0	0	0	$-\frac{1}{4}$	0	1	2
$G49$	0	0	0	0	0	0	0	$\frac{3}{4}$	0	0	1	0	4
$G50$	0	0	-1	0	0	0	0	0	$\frac{3}{2}$	0	0	0	0
$G51$	0	0	0	$-\frac{3}{4}$	0	0	0	0	0	$\frac{1}{2}$	0	0	4
$G52$	0	0	0	0	$\frac{1}{2}$	0	0	0	0	$\frac{1}{4}$	0	0	4
$G53$	0	$\frac{1}{2}$	0	0	0	0	0	0	2	0	0	0	0
$G54$	0	0	-2	0	0	0	0	0	1	0	0	0	0
$G55$	0	0	0	$-\frac{3}{4}$	0	0	0	0	0	$\frac{1}{2}$	0	-1	2
$G56$	0	$\frac{1}{2}$	0	0	0	0	0	0	0	0	0	0	0
$G57$	0	0	0	0	0	$\frac{1}{4}$	0	0	0	$-\frac{1}{4}$	$-\frac{1}{2}$	$-\frac{3}{4}$	$\frac{9}{2}$
$G58$	0	0	0	0	$\frac{1}{2}$	0	0	0	0	0	0	1	4
$G59$	0	0	0	0	0	$\frac{1}{2}$	0	0	0	0	-1	0	0
$G60$	0	0	0	0	$\frac{1}{2}$	0	0	0	0	$\frac{1}{2}$	0	1	-2
$G61$	0	1	0	0	0	0	0	0	-2	0	0	0	0
$G62$	0	0	0	$-\frac{3}{4}$	0	0	0	0	0	0	0	$-\frac{3}{2}$	-3
$G63$	0	0	0	0	$\frac{1}{4}$	0	0	0	0	$-\frac{1}{4}$	0	0	0
$G64$	0	0	0	0	0	$\frac{1}{2}$	0	0	0	0	0	0	0
$G65$	0	0	0	0	$\frac{1}{2}$	0	0	0	0	$-\frac{1}{2}$	0	1	2
$G66$	0	1	0	0	0	0	0	0	2	0	0	0	0
$G67$	0	0	0	0	0	0	0	$\frac{1}{4}$	0	0	0	0	0
$G68$	0	0	-1	0	0	0	0	0	0	0	0	0	0
$G69$	-1	0	0	0	0	0	0	0	0	0	0	0	0

Table 1 Weak-Expansion of Invariants with (Mass)⁶-Dim.: $(\partial\partial h)^3$ -Part

G43-G69(l=3)

Graph	P_1	P_2	P_3	P_4	P_5	P_6	A_1	B_1	T_1	T_2	T_3	T_4	S
$G70$	0	0	0	$\frac{1}{8}$	0	0	0	0	0	$-\frac{1}{4}$	0	0	4
$G71$	0	0	0	0	$-\frac{1}{4}$	0	0	0	0	$-\frac{1}{8}$	0	$-\frac{1}{2}$	-2
$G72$	0	0	1	0	0	0	0	0	$-\frac{3}{2}$	0	0	0	0
$G73$	0	0	0	$\frac{3}{8}$	0	0	0	0	0	$-\frac{1}{2}$	0	0	4
$G74$	0	-1	0	0	0	0	0	0	2	0	0	0	0
$G75$	0	0	0	0	$-\frac{1}{4}$	0	0	0	0	$-\frac{1}{2}$	0	$-\frac{1}{2}$	3
$G76$	0	$-\frac{1}{4}$	0	0	0	0	0	0	1	0	0	0	0
$G77$	0	0	0	$\frac{1}{8}$	0	0	0	0	0	0	0	$\frac{1}{4}$	$\frac{1}{2}$
$G78$	0	0	0	0	$-\frac{1}{4}$	0	0	0	0	$\frac{1}{8}$	0	$-\frac{1}{2}$	-1
$G79$	0	$-\frac{1}{4}$	0	0	0	0	0	0	$-\frac{1}{2}$	0	0	0	0
$G80$	0	0	0	$\frac{3}{8}$	0	0	0	0	0	$-\frac{1}{4}$	0	$\frac{1}{4}$	$-\frac{1}{2}$
$G81$	0	-1	0	0	0	0	0	0	-2	0	0	0	0
$G82$	0	0	0	0	$-\frac{1}{4}$	0	0	0	0	$-\frac{1}{4}$	0	$-\frac{1}{2}$	1
$G83$	0	$-\frac{1}{2}$	0	0	0	0	0	0	1	0	0	0	0
$G84$	0	0	1	0	0	0	0	0	0	0	0	0	0
$G85$	3	0	0	0	0	0	0	0	0	0	0	0	0
$G86$	0	$\frac{1}{4}$	0	0	0	0	0	0	-1	0	0	0	0
$G87$	0	$\frac{1}{4}$	0	0	0	0	0	0	$\frac{1}{2}$	0	0	0	0
$G88$	-3	0	0	0	0	0	0	0	0	0	0	0	0
$G89$	0	$\frac{1}{2}$	0	0	0	0	0	0	-1	0	0	0	0
$G90$	1	0	0	0	0	0	0	0	0	0	0	0	0

Table 1 Weak-Expansion of Invariants with (Mass)⁶-Dim.: $(\partial\partial h)^3$ -Part

$G70\text{-}G85(l=4), G86\text{-}G89(l=5), G90(l=6)$

References

[1] L.Alvarez-Gaumé and E.Witten, Nucl.Phys. **B234**, 269 (1983).

- [2] L.Bonora,P.Pasti and M.Bregola,Class.Quantum.Grav.**3**,635(1986).
- [3] S. Deser, Uniqueness of D=11 Supergravity, hep-th/9712064,Lecture at ‘Quantum Mechanics of Fundamental Systems VI’,Santiago,Chile,August 1997.
- [4] S.Ferrara and B.Zumino,Nucl.Phys.**B87**,207(1975).
- [5] J.Schwinger,Phys.Rev.**82**,664(1951).
- [6] B.DeWitt,Dynamical theory of groups and fields,Gordon and Breach, New York,1965.
- [7] R.T.Seeley,Proc.Symp.Pure Math.**10**,Amer.Math.Soc.,(1967)288.
- [8] F.Bastianelli,Nucl.Phys.**B376**,113(1992).
- [9] F.Bastianelli and P. van Nieuwenhuizen,Nucl.Phys.**B389**,53(1993).
- [10] J.de Boer,B.Peeters,K.Skenderis and P. van Nieuwenhuizen, Nucl.Phys.**B446**,211(1995).
- [11] J.de Boer,B.Peeters,K.Skenderis and P. van Nieuwenhuizen, Nucl.Phys.**B459**,631(1996).
- [12] G.'tHooft,Nucl.Phys.**B62**,444(1973).
- [13] G. t'Hooft and M. Veltman, *Ann.Inst.H.Poincaré* **20** (1974) 69.
- [14] P.B.Gilkey,J.Diff.G geom.**10**,601(1975).
- [15] I.G.Avramidi, The covariant methods for calculation of the effective action in quantum field theory and the investigation of higher derivative quantum gravity, PhD Thesis, Moscow State Univ.,Moscow,1986; hep-th/9510140
- [16] I.G.Avramidi,Nucl.Phys.**B355**,712(1991).
- [17] A.O.Barvinsky and G.A.Vilkovisky,Phys.Rep.**C119**,1(1985).
- [18] S.Yajima,Class.Quantum Grav.**14**,2853(1997).
- [19] I.L.Buchbinder,S.D.Odintsov and I.L.Shapiro,Effective Action in Quantum Gravity,IOP Pub.,1992.
- [20] Other examples of the coordinate space approach are the operator expansion method and the lattice field theory. The former was exploited in the 2 dim conformal field theory.
- [21] The heat-kernel is formulated in the coordinate space, using the quantum-mechanical non-linear sigma model, and the Feynman rules are given in [8, 9, 10, 11].

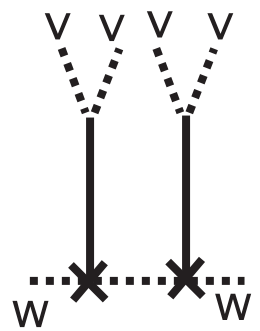
- [22] S.Ichinose and N.Ikeda,Phys.Rev.**D53**,5932(1996).
- [23] It must be compared with the dimensional regularization.
- [24] K.Fujikawa,Nucl.Phys.**B226**,437(1983).
- [25] K.Fujikawa,Phys.Rev.Lett.**42**,1195(1979);**44**,1733(1980);
Phys.Rev.**D21**,2848(1980);**D22**,1499(E)(1980).
- [26] K.Fujikawa,Lecture in Quantum Gravity and Cosmology, Kyoto Summer Inst.1985,ed. by Sato and Inami,World Scientific :106 (1985) ; This is the good review of the series of works by Fujikawa.
- [27] E.Abdalla, M.C.B.Abdalla and K.D.Rothe,*Non-perturbative Methods in 2 Dimensional Quantum Field Theory*(World Scientific,Singapore, 1991).
- [28] E.D'Hoker,*Tasi Lectures on Critical String Theory*, UCLA/92/TEP/30(1992).
- [29] S.Ichinose and N.Ikeda,DAMTP/96-87, hep-th/9610136, "Gauge Symmetry of the Heat Kernel and Anomaly Formulae".
- [30] The case of special $W_{\mu\nu}^{ij}$ (Riemann geometry) was done by Gilkey[14], where he analyzed using the normal coordinates in order to keep the general covariance manifestly.
- [31] J.D.Bjorken and S.D.Drell,*Relativistic Quantum Mechanics* (McGraw-Hill,New York,1964).
- [32] O.Alvarez,Nucl.Phys.**B216**,125(1983).
- [33] The condition $t > 0$ in $G_0(x - y; t)$ requires the directedness.
- [34] These properties come only from the physical dimensions of $W_{\mu\nu}$, N_μ and M , not the speciality of the present model. The relevant-part selection in this section is valid for general theories.
- [35] The divergent parts t^{-1}, t^{-2}, \dots are considered to be canceled by the divergent counter-terms. They generally correspond to power-divergences (not log-divergence) and the counter-terms are those operators which have massive couplings: ex. the cosmological term, the Einstein term.
- [36] The \bar{w}^8 -term gives disconnected graphs, and \bar{w}^6 -terms give graphs which conflict with the second one of the common features of Graph3 and 67.
- [37] S.Ichinose, Int.J.Mod.Phys.**C9**,243(1998),hep-th/9609014
- [38] M.J.Duff,Nucl.Phys.**B125**(1977)334
- [39] S.Deser and A.Schwimmer,Phys.Lett.**B309**(1993)279.

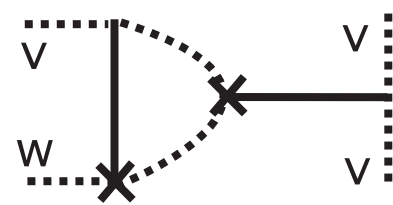
- [40] S.Ichinose ,US-97-08, hep-th/9801056, "General Structure of Conformal Anomaly and 4 Dimensional Photon-Dilaton Gravity".
- [41] S.A.Fulling, R.C.King, B.G.Wybourne and C.J.Cummins, Class.Quantum.Grav.,**9**,1151(1992)
- [42] S.Ichinose,Class.Quantum Grav.**12**,1021(1995).
- [43] The total independent $(\partial\partial h)^3$ -terms are given by 90 terms shown in the first column of the table in App.D.
- [44] M.B.Green and J.H.Schwarz,Phys.Lett.**149B**,117(1984).
- [45] M.J.Duff,Class.Quantum Grav.**11**,1387(1994).
- [46] S.Ichinose and N.Ikeda,J.Math.Phys.**38**,6475(1997).

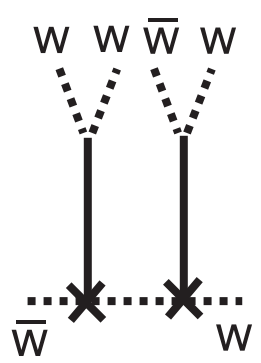
Figure Captions

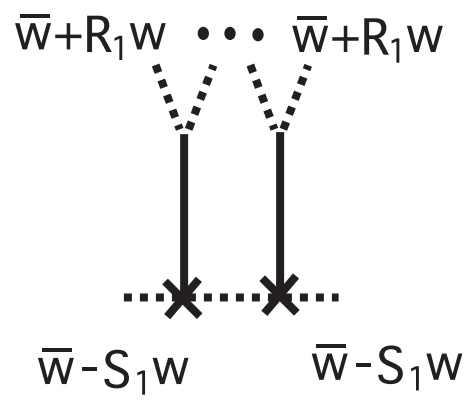
- Fig.1 Graph of $G_0(x - y; t)$
- Fig.2 Graph of $G_1(x, y; t)$
- Fig.3 Graph of $G_2(x, y; t)$
- Fig.4 Graph of $G_3(x, y; t)$
- Fig.5 Graph of $G_0(0; t)$
- Fig.6 Graph of $G_1(x, x; t)$
- Fig.7 Graph of $G_2(x, x; t)$
- Fig.8 Graph of $G_3(x, x; t)$
- Fig.9 Four Graphs of 3,67,1 and 2. See the (40) for the definition of the graph.
- Fig.10 Two important $(\partial\partial h)^4$ -graphs in 8 dim.
- Fig.11 Two important $(\partial\partial h)^5$ -graphs in 10 dim.
- Fig.12 Propagator Rule 1, Eq.(59).
- Fig.13 Propagator Rule 2, Eq.(60).
- Fig.14 Propagator Rule 3, Eq.(61).
- Fig.15 Propagator Rule 4, Eq.(62).
- Fig.16 $W^{\mu\nu}$ and N_λ .
- Fig.17 M , Order of h .
- Fig.18 M , Order of h^2 .
- Fig.19 M , Order of h^3 and loop no=2.
- Fig.20 M , Order of h^3 and loop no=1.
- Fig.21 M , Order of h^3 and loop no=0.

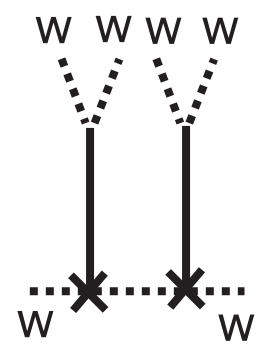
✗.....✗.....✗

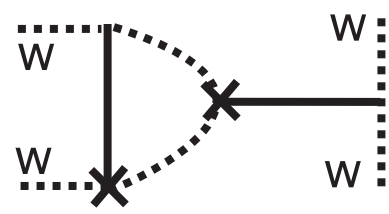


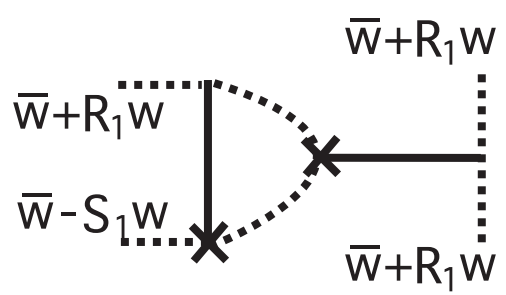


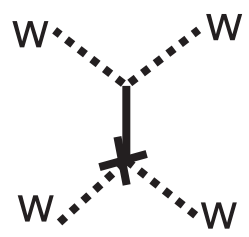




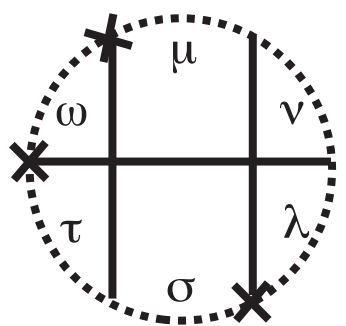








$$\begin{array}{ccc} \bar{w} + R_1 w & & \bar{w} + R_1 w \\ & \searrow & \swarrow \\ & \downarrow & \\ \bar{w} - S_1 w & & \bar{w} - S_1 w \end{array}$$



Graph 7